JMCC7818-R2

Differential Roles of Cardiac and Leukocyte Derived Macrophage Migration Inhibitory Factor in Inflammatory Responses and Cardiac Remodelling Post Myocardial Infarction

[1,4]David A White, B.Sc(Hons), [1]Yidan Su, PhD., [1]Peter Kanellakis, B.Sc(Hons), [1]Helen Kiriazis, PhD., [2]Eric F Morand, MD, PhD., [3]Richard Bucala, MD, PhD., [1,4,5]Anthony M. Dart, FRACP, DPhil., [1,5]Xiao-Jun Du, PhD., [1,6]Xiao-Ming Gao, MD.

[1]Baker IDI Heart and Diabetes Institute, Australia

[2]Centre for Inflammatory Diseases, Southern Clinical School, Monash University, Australia

[3]Yale University School of Medicine, New Haven, Connecticut, USA

[4]Department of Cardiovascular Medicine, Alfred Hospital, Australia

[5]Department of Medicine, Central Clinical School, Monash University, Australia

[6]Department of Surgery, Central Clinical School, Monash University, Australia

Short title: MIF promotes inflammation following MI

Word count: **8,710** Abstract: **240** Figures: **6** Tables: **2**

#1 Correspondence to
Dr: Xiao-Ming Gao
Baker IDI Heart and Diabetes Institute,
75 Commercial Road,
Melbourne 3004, Victoria, Australia
Telephone: 61-3-85321295
Facsimile: 61-3-85321100
Email: xiaoming.gao@bakeridi.edu.au

#2 Correspondence to
A/Prof: Xiao-Jun Du
Baker IDI Heart and Diabetes Institute,
75 Commercial Road,
Melbourne 3004, Victoria, Australia
Telephone: 61-3-85321267
Facsimile: 61-3-85321100
Email: xiao-jun.du@bakeridi.edu.au

Abstract

Myocardial infarction (MI) provokes regional inflammation which facilitates the healing, whereas excessive inflammation leads to adverse cardiac remodelling. Our aim was to determine the role of macrophage migration inhibitory factor (MIF) in inflammation and cardiac remodelling following MI.

Wild type (WT) or global MIF deficient (MIFKO) mice were subjected to coronary artery occlusion. Compared to WT mice, MIFKO mice had a significantly lower incidence of post-MI cardiac rupture (27% vs. 53%) and amelioration of cardiac remodelling. These were associated with suppressed myocardial leukocyte infiltration, inflammatory mediators' expression, and reduced activity of MMP-2, MMP-9, p38 and JNK MAPK. Infarct myocardium-derived or exogenous MIF mediated macrophage chemotaxis *in vitro* that was suppressed by inhibition of p38 MAPK or NF-κB. To further dissect the role of MIF derived from different cellular sources in post-MI cardiac remodelling, we generated chimeric mice with MIF deficiency either in bone marrow derived-cells (WT^{KO}) or in somatic-cells (KO^{WT}). Compared to WT and KO^{WT} mice, WT^{KO} mice had reduced rupture risk and ameliorated cardiac remodelling, associated with attenuated regional leukocyte infiltration and expression of inflammatory mediators. In contrast, KO^{WT} mice had delayed healing and enhanced expression of M1 macrophage markers, but diminished expression of M2 markers during the early healing phase.

In conclusion, global MIF deletion protects the heart from post-infarct cardiac rupture and remodelling through suppression of leukocyte infiltration and inflammation. Leukocyte-derived MIF promotes inflammatory responses after MI, whereas cardiac-derived MIF affects early but not ultimate healing process.

Key words: macrophage migration inhibitory factor; myocardial infarction; inflammation, healing

Introduction

Myocardial infarction (MI) is the leading cause of cardiac death worldwide and its occurrence is expected to increase with population aging [1]. A great challenge to modern cardiology is to limit cardiac damage and prevent adverse left ventricular (LV) remodelling and dysfunction after MI [2, 3]. Many studies on the role of inflammatory responses to MI have highlighted the dual nature of the contribution of inflammation to disease progression. Following myocardial ischemia, necrotic cardiomyocytes release a wide range of inflammatory molecules such as reactive oxygen species and cytokines that stimulate regional inflammatory infiltration [4]. Recruitment of leukocytes to the injured myocardium is essential for healing via phagocytosis of cellular debris, activation of matrix metalloproteinases (MMPs) to remodel extracellular matrix (ECM), and secretion of growth factors to promote granular angiogenesis and deposition of ECM proteins [5, 6]. However, either excessive or inadequate inflammation in the injured myocardium can lead to adverse outcomes such as cardiac rupture, adverse ventricular remodelling and heart failure [6, 7].

Macrophage migration inhibitory factor (MIF) is a pleiotropic cytokine with a number of unique biological actions and is recognised as an important regulator of innate and acquired immunity [8, 9]. Pro-inflammatory actions of MIF have been reported in various inflammatory diseases such as sepsis, rheumatoid arthritis and atherosclerosis [9-11]. MIF is released from intracellular stores in response to various cellular stressors, such as hypoxia or bacterial proteins [12]. MIF is rapidly released from the heart, if subjected to a brief period of ischemia, and enhances glucose uptake via activation of AMP-activated protein kinase (AMPK) [13, 14], whilst it also inhibits c-Jun N-terminal kinase (JNK) [15] and attenuates oxidative stress [16], thereby reducing infarct size and preserving cardiac function. However, prolonged ischemia, which is frequently seen in clinical practice [1], provokes severe cardiac inflammatory responses. We recently reported that prolonged ischemia in mice leads to substantial myocardial damage and regional inflammation, effects which

are attenuated in mice with a global MIF deletion (MIFKO) [17]. These distinct observations of the effects of MIF in different contexts highlight the complexity of pathophysiological processes following ischemic cardiac injury and warrant further investigations on the role of MIF, especially when anti-MIF therapies are to be considered for MI.

In the current study, we investigated the phenotype of MIFKO mice subjected to MI, by measuring post-MI inflammation, healing, and acute and chronic cardiac remodelling. MIF is expressed in multiple cell types including both leukocytes [18] and cardiomyocytes [19], but the relative contributions of these sources of MIF to myocardial injury are unknown. We hypothesized that MIF derived from different cellular sources would have different effects in the heart following ischemic injury. This hypothesis was investigated in chimeric mice generated by bone marrow transplant. The results confirm that MIF plays a vital role in mediating cardiac inflammatory injury after MI, and show that while leukocyte MIF enhances damage, non-leukocyte MIF enhances myocardial healing.

Methods

A detailed methodology section can be found in the online supplemental materials

Animals

All animal investigations were approved by a local animal ethics committee complying with the Australian Code of Practice for the Care and Use of Animals for Scientific Purposes (7^{th} edition). Ten-week-old male global MIFKO mice and wild type (WT) littermates with C57Bl/6 genetic background were used [20].

Induction of MI

Mice underwent coronary artery occlusion to induce MI or sham operation, as previously described [21, 22]. After surgery, mice were monitored daily for 4 weeks. Autopsy was performed for evidence of post-MI cardiac rupture or heart failure, as described previously [22]. Mice were killed at various time points following MI, infarct size was assessed and infarct and non-infarct myocardium were separated, snap frozen in liquid nitrogen and stored at -80°C for molecular assays. Further, some LVs were fixed in 10% formalin or fresh frozen for histological analyses.

Echocardiography

Echocardiography was performed prior to surgery and 1, 2 or 4 weeks post-surgery, as previously described [17, 23].

Immunofluorescence staining

Immunofluorescence was performed, as previously described [17]. Briefly, LV sections were stained with an anti CD45 antibody for leukocyte, and 4', 6-diamidino-2-phenylindole (DAPI) for nucleus, to identify leukocytes. Visualisation of capillaries in border zones was performed using

Alexa Fluor® 568 isolectin GS-IB_4 conjugate. Images were acquired using an Olympus BX61 fluorescence microscope and densities of leukocytes and capillaries were analysed using Image Pro Plus software (Media Cybernetics, Inc, USA).

Quantitative real time-PCR

RNA was extracted from cardiac tissues. Gene expression of monocyte chemotactic protein-1 (MCP-1), intercellular adhesion molecule-1 (ICAM-1), vascular cell adhesion molecule 1 (VCAM-1), interleukin-1β (IL-1β), IL-10, MMP-9, MMP-2 and transforming growth factor β1 (TGFβ1) was assessed by quantitative real-time PCR (qPCR) using Applied Biosystems 7500 fast real-time PCR system and normalised to GAPDH, as previously described [17, 24].

Enzyme linked immunosorbent assay

Enzyme-linked immunosorbent assay (ELISA) was performed, in duplicates, using a commercial mouse IL-1β (Life Research, Australia) and MIF (ElAab Science Co. Ltd. Wuhan, China) ELISA kits according to the manufactures' instructions.

Gelatin zymography

Proteins were extracted from infarct tissues and sham-operated hearts and concentrations were determined using Bradford protein quantification assay. Gelatin zymography was performed on a 7.5% acrylamide, 0.5% gelatine SDS page, as previously described [24].

Immunoblotting

Western blotting was performed with primary antibodies to phospho- and total-p38 mitogen-activation protein kinase (p-p38 and t-p38 MAPK), p-JNK and t-JNK, as reported previously [17]. Membranes were re-probed with GAPDH antibody to verify loading consistency.

Histology

Formalin-fixed paraffin-embedded LV sections were stained for hemotoxylin and eosin to assess remaining necrotic areas and scar thickness while picosirius red was used to determine collagen deposition in the infarct region. Images were captured on using an Olympus light microscope and analysed using Image-Pro Plus 6.0 software, as described previously [21, 25].

Cell culture experiments.

To further understand potential influence of MIF on post-infarct healing, we studied effects of MIF on cardiac fibroblast biology in cell culture models. First, we examined whether fibroblasts and cardiomyocytes are able to release MIF under hypoxic stimulation. Second, fibroblasts were prepared from the infarct tissue of adult MIFKO and WT mice subjected to MI for 4 days, fibroblast proliferation, collagen deposition and fibrosis-related gene expression including TGFβ, α-smooth muscle actin (α-SMA), collagen-1 and -3 were investigated.

Trans-well migration assay

Macrophages were isolated from the peritoneal cavities of WT and global MIFKO mice. Using a trans-well migration assay, cells were exposed to homogenised infarct or normal cardiac tissue, or recombinant human MIF (rMIF). Additionally, WT macrophages were pre-treated with either a p38 MAPK inhibitor, SB203580, or NF-κB inhibitor, Bay11-7082, prior to migration assay. The number of trans-well migrated macrophages was counted.

Generation of chimeric mice

A detailed description of the bone marrow transplantation (BMT) of WT and global MIFKO mice can be found in the Online Supplemental Material. Briefly, after lethal irradiation (550 rads twice), WT mice received bone marrow from MIFKO mice via a tail vein injection to create (WT^{KO}) mice with MIF deficiency in bone marrow derived cells (or leukocytes). In parallel, irradiated MIFKO

mice received WT bone marrow to create (KO^{WT}) mice deficient in MIF in somatic cells (or the heart). After BMT, animals were allowed to recover for 4 weeks before coronary artery ligation or sham operation. Chimeric mice were monitored up to 2 weeks after surgery. Echocardiography, immunofluorescence, histology and qPCR for gene expression of MIF, M1 macrophage markers [IL-1β, interferon-γ (IFN-γ), tumor necrosis factor α (TNFα, IL-6] and M2 macrophage markers [TGFβ1, arginase 1 (Arg-1), macrophage mannose receptor 1 (MRC-1) and CD163] [26] were performed as described above. To confirm success of BMT, peripheral blood cells were collected and purified using Maxwell DNA extraction and genotyped (Online Figure 1).

To clarify the potential influence of irradiation on observed phenotypes, we reconstituted WT bone marrow to irradiated WT mice (WT^{WT}), or MIFKO bone marrow to irradiated MIFKO mice (KO^{KO}), then subjected mice to coronary artery occlusion. Incidence of cardiac rupture within 2 weeks was investigated.

Statistics

Results are presented as mean±SEM unless otherwise stated. Graphpad Prism software (version 5.0) was used for the statistical analysis. Survival was analysed by Kaplan-Meier analysis and compared by the log-rank, Chi-square or Fisher exact test. One- or two-way analysis of variance (ANOVA) followed by Newman-Keuls *post-hoc* tests were used to detect differences between groups. $P<0.05$ was considered statistically significant.

.

Results

Global MIF deficiency improved survival by reducing post-MI cardiac rupture

At 4 weeks after MI, survival was much better in MIFKO (66%) than WT littermates (45%, *P<0.05*, Figure 1A). Over the first week, significantly more WT than MIFKO mice died of cardiac rupture (*P<0.05)* (Figure 1B), indicating deleterious effects of MIF on cardiac rupture post MI. Typically, cardiac rupture occurred during 3-6 days following MI, consistent with our previous reports [22, 27]. One WT and two MIFKO mice developed heart failure and were killed prematurely in the second week, the remaining mice were killed at 4 weeks post MI. Infarct size was comparable between WT and MIFKO mice, when measured at autopsy in those mice dying of rupture within 3-5 days (acute phase) and in surviving mice at 4 weeks post MI (chronic phase, Figure 1C).

Global MIF deficiency ameliorated post-MI cardiac remodelling

Echocardiography prior to MI revealed no significant differences in cardiac dimensions and function between WT and MIFKO mice. At week-1 and week-4 following MI, WT and MIFKO mice displayed gradually increasing LV dimensions and decreasing fractional shortening (FS) when compared with baseline values (Figure 1D). However, MIFKO mice had significantly smaller LV dimensions and better FS when compared to WT group at 4 weeks following MI (*P<0.05*, Figure 1D, Online Table 1). These results indicate that MIF contributes to adverse cardiac remodelling post MI.

Global MIF deficiency had moderate influence on healing

We next investigated the effect of global MIF deletion on post-infarct healing. The fractional size of remaining necrotic area in the infarct region was reduced between 7 to 14 days to a similar extent in both WT (13% to 3%) and MIFKO mice (17% to 2%). No significant difference was observed

between genotypes at either time point following MI (Online Figure 2A and 2B). Between 7 and 14 days post-MI, collagen content in the infarct region was increased in both WT (24% to 59%) and MIFKO mice (19% to 48%), but collagen content was significantly lower in MIFKO mice at 14 days (*P<0.05* vs. WT, Online Figure 2C and 2D). Capillary densities in the infarct border zone were comparable between WT and MIFKO mice at 7 and 14 days following MI (Online Figure 2E and 2F). Expression of TGFβ1 mRNA was similarly increased (~6.5-fold) at day-1 and day-7 post-MI in MIFKO and WT mice, but 30% higher in WT versus MIFKO mice at day-3 when the expression reached its maximum (*P<0.05,* Online Figure 2G). Infarct wall thickness at 7 and 14 days following MI was lower versus sham values in both WT and MIFKO mice, and the thickness was significantly greater in MIFKO than WT mice at day-14 post-MI (*P<0.05,* Online Figure 2H).

We further studied potential influence of MIF on cardiac fibroblast biology by in vitro cell culture experiments. First, 6 h hypoxia exposure induced substantial release of MIF from cardiomyocytes with a similar trend in fibroblasts (Online Figure 3A). Second, we dissected and cultured fibroblasts for 48 h from the infarct tissue of both global MIFKO and WT mice at day-4 after MI, and found that cell proliferation was 28% in MIFKO and 47.2% in WT group (*P<0.05*) compared with their respective baseline levels (Online Figure 3B). Collagen deposition by cardiac fibroblasts was 3% lower in MIFKO than in WT mice (7% vs. 10%, *P=NS*) over their respective baseline levels (Online Figure 3C). There was no difference in mRNA levels of TGFβ and α-SMA between MIFKO and WT mice. Collagen-1 expression was significantly higher in MIFKO than that in WT fibroblasts while there was a trend to lower collagen-3 expression in MIFKO fibroblasts (Online Figure 3D). These data suggest that global MIF deficiency may not impact on early healing post MI albeit MIF deficiency decreased proliferation of cardiac fibroblasts post MI.

Global MIF deficiency attenuates acute inflammatory responses post MI

As regional inflammation following MI leads to tissue damage contributing to subsequent cardiac remodelling, we next investigated the effect of global MIF deletion on temporal changes in

leukocyte infiltration and expression of pro-inflammatory mediators post-MI.

Immunohistochemistry for CD45, a marker of leukocytes, revealed increased leukocyte density in the infarct region including the border zone in both genotypes from 6 h to 7 days following MI (Figure 2B). In WT mice, leukocyte density peaked at day-3 and declined by day-7. Compared to WT mice, MIFKO mice had significantly lower leukocyte density in the infarct myocardium at days 1-3 (both $P<0.05$) (Figure 2A and 2B). In addition, expression of MCP-1, ICAM-1, VCAM-1 and IL-1β mRNA in the infarct tissue of both WT and MIFKO mice was significantly increased over sham values at multiple time points (Figure 2C-F), with a significantly lower expression level in MIFKO mice at 24 h and day-3 ($P<0.05$, Figure 2C-F). Expression of the anti-inflammatory cytokine, IL-10, was also increased in both groups as early as 6 h post-MI and it was markedly higher in MIFKO than WT heart at day-3 (Figure 2G, $P<0.05$). To assess whether global MIF deletion also influences systemic inflammatory responses, we measured plasma concentrations of IL-1β by ELISA. Plasma IL-1β was significantly elevated above baseline in WT mice at 24 h, and MIFKO mice had significantly lower plasma IL-1β levels at 6 and 24 h following MI (Figure 2H, $P<0.05$).

Global MIF deficiency reduces MMP activity following MI

As excessive activation of MMPs has been implicated in adverse cardiac remodelling [28], we also measured mRNA expression and activity of MMP-9 and MMP-2 by qPCR and gelatine zymography. Both expression and activity of MMP-9 and MMP-2 were at very low levels in sham WT or MIFKO hearts (Figure 3A-C). Following MI, MMP-9 expression and activity increased from 24 h to day-3 in WT hearts with a blunted response in MIFKO mice (Figure 3A-C). Abundance, mRNA level and activity of MMP-2 were significantly increased until day-7 post-MI but with attenuated MMP-2 expression and activity in MIFKO hearts ($P<0.05$, Figure 3A-C).

Global MIF deficiency attenuates MI induced phosphorylation of p38 MAPK and JNK

To elucidate how MIF regulates inflammatory signalling following MI, we performed immunoblotting for p38 and JNK MAPK, both are important in inflammatory signalling post MI [29-31]. There was no difference between sham-operated WT and MIFKO groups in levels of phosphorylated p38 or JNK (Figure 4A and 4B). At day-3 following MI, phosphorylation of both p38 MAPK and JNK was significantly elevated in both genotypes with such increment significantly attenuated in MIFKO infarct hearts ($P<0.05$, Figure 4A and B).

MIF mediates macrophage migration to the infarct myocardium

To seek direct evidence for MIF promoting inflammatory infiltration, we tested, using an *ex vivo* trans-well migration assay [18], migration of peritoneal macrophages prepared from WT or global MIFKO mice in response to homogenised infarct myocardium. Macrophages from either genotype displayed a similar and minimal migration to homogenised sham-operated cardiac tissue of WT or MIFKO mice (Figure 4C). WT macrophages showed a 4-fold increase in migration in response to homogenised WT infarct tissue, but significantly attenuated in response to MIFKO infarct tissue (Figure 4C). Moreover, addition of anti-MCP-1 monoclonal antibody to the WT infarct tissue homogenate significantly inhibited migration (Figure 4C). When MIFKO macrophages were exposed to WT infarct tissue, migration was also lower than WT macrophages, and cell migration was further reduced when MIFKO macrophages were exposed to MIFKO infarct tissue (Figure 4C). To confirm the chemoattractant property of MIF, rMIF was added to the lower chamber and the top chamber loaded with WT macrophages. We observed a dramatic macrophage migration (Figure 4D) under these conditions i.e. in the absence of other chemotracttants such as would be found in the infarct tissue. To further illustrate mechanisms involved in MIF-mediated macrophage migration, we investigated effects of specific inhibitors on the macrophage migration evoked by rMIF. Compared with control media, rMIF induced significant migration of WT macrophages, which was partially or largely inhibited by pre-treatment of WT macrophages with the p38 MAPK inhibitor, SB203580, or the NF-κB inhibitor, Bay11-7082 (Figure 4D).

Bone marrow derived-cell MIF deficiency (WT^{KO}) lowers risk of cardiac rupture and ameliorates cardiac remodelling post-MI

As MIF is derived from both the myocardium and immune cells [8, 14], we next investigated the respective roles of MIF derived from different cellular sources on post-MI inflammation and cardiac remodelling. Chimeric mice were created with MIF deficiency either in somatic-cells (KO^{WT}) or in bone marrow derived-cells (WT^{KO}) (confirmation of genotype, Online Figure 1). Compared with WT counterparts (serving as the baseline control), KO^{WT} mice had only a slight reduction in the incidence of cardiac rupture. In contrast, WT^{KO} mice had a significantly reduced occurrence of rupture events which was even lower than that in MIFKO mice (Figure 5A and 5B). Interestingly, while the time window for rupture was slightly prolonged in WT^{KO} mice it was significantly extended in KO^{WT} compared to WT mice ($P<0.05$, Figure 5A) [22, 27]. Further, echocardiography revealed that relative to leukocyte-MIF deficient or WT mice, KO^{WT} mice displayed greater LV end-diastolic dimension and lower FS when studied at day-7 and day-14 post-MI (Table 1).

To clarify the potential effect of irradiation on observed phenotypes in chimeric mice, we reconstituted WT bone marrow to irradiated WT mice (WT^{WT}), or global MIFKO bone marrow to irradiated MIFKO mice (KO^{KO}), and then subjected these mice to MI. We observed that rate and time-window of cardiac rupture as well as infarct size (data not shown) were comparable between KO and KO^{KO}, or between WT and WT^{WT} mice (Online Figure 4), indicating that irradiation had minimal influence on the phenotypes observed.

Somatic-cell MIF deficiency (KO^{WT}) delays wound healing following MI

We further examined the impact of cardiac- or leukocyte-MIF deficiency on the healing process by determining the size of residual necrotic area, collagen deposition, infarct wall thickness and capillary densities. Residual necrotic area was markedly reduced in WT, KO^{WT} and WT^{KO} mice

during 7 to 14 days post-MI. However, KO^{WT} mice had much greater necrotic area than WT or WT^{KO} mice at day-7, although no difference remained by day-14 after MI (Table 2). While infarct wall thickness was reduced by 40-50% in all 3 groups from 7 to 14 days, a thicker infarct wall was observed in KO^{WT} mice at 14 days post-MI (Table 2). In contrast, compared to sham-operated hearts of all 3 genotypes (data not shown), there was a marked increase in collagen density in the infarct region in WT mice which was significantly abrogated in both chimeric groups at day-7 post-MI (Table 2). At day-14, while collagen density was further increased in all 3 groups it remained lower in both chimeric groups with a more significant reduction in KO^{WT} than WT^{KO} mice ($P<0.05$, Table 2). Capillary densities in sham-operated hearts were comparable among the 3 groups, but increased from 7 to 14 days post-MI in WT and WT^{KO} mice, whereas in KO^{WT} mice significantly less increase in capillary density was observed (Table 2). These data suggest a delayed infarct healing in those mice with MIF deficiency in somatic cells but still expressing MIF in bone marrow-derived cells. However by examining these healing-related parameters at 4 weeks after MI, we found there was no difference in collagen content (69±4% vs. 68±5%) or wall thickness (293±22 vs. 290±16 μm) between WT^{KO} and KO^{WT} group. Clearance of necrotic tissues was also complete in both groups. These indicated that although somatic cell/cardiac MIF deficiency delayed the healing process acutely, chronic healing was not impaired.

MIF expressed in the heart by different cells differentially influences leukocyte infiltration

Immunohistochemical staining revealed a temporal change of infiltrating leukocytes in the infarct myocardium including the border zone in chimeric mice following MI. Although similarly lower versus WT values at day-3 following MI, leukocyte densities in both chimeric groups were markedly increased at day-3 from respective sham values (Figure 5C). Compared to the peak level at day-3 in WT mice, both KO^{WT} and WT^{KO} mice had a lower leukocyte density at the same time point, but peaked at day-7 then declined by day-14 post-MI, corresponding with the extended time window for rupture that was observed (Figure 5A and 5C). Interestingly, KO^{WT} mice displayed

increased leukocyte infiltration at day-7 post MI compared to WT^{KO} and WT mice. There were no differences in leukocyte density in the infarct region at day-14 among the 3 groups (Figure 5C).

To explore the linkage between MIF expression and inflammatory cell infiltration, we studied MIF gene and protein expression in the infarct myocardium at similar time points following MI. There was no difference in MIF gene expression between sham-operated WT and WT^{KO} mice, whereas MIF expression in KO^{WT} mice was undetectable (Figure 5D). Following MI, MIF mRNA levels in WT mice were considerably increased and sustained up to 14 days with the peak at day-3, consistent with the temporal pattern of leukocyte infiltration (Figure 5C and D). In WT^{KO} mice, although leukocyte infiltration steadily increased after MI with a peak at day-7 with maintained elevation till day-14 (all $P<0.05$ vs. sham), MIF mRNA levels did not change during the 2-week study period (Figure 5C and D). In KO^{WT} mice, leukocyte density was significantly increased post MI with a peak at day-7 and then a reduction by day-14 with corresponding upregulation of MIF expression at day-3 and day-7 and significant decrease at day-14 (Figure 5C and D). Notably, although the absolute MIF mRNA level in KO^{WT} mice with MI was significantly lower than other two genotypes, the increment at day-3 and day-7 relative to KO^{WT} sham level (undetectable) was remarkable (Figure 5D). Among the 3 groups, elevation of MIF mRNA level was the highest in WT. Intriguingly, when adding up MIF mRNA values from WT^{KO} and KO^{WT} groups, it was very close to the WT values at day-3 and day-7 post-MI (Figure 5D), indicating that leukocytes are also an important cellular source of regional MIF. Meanwhile Western blotting revealed a different pattern in MIF protein expression. At day-3 post-MI, MIF content in the infarct myocardium of WT and WT^{KO} mice was significantly reduced by approximately 50% compared to their respective sham values, but was restored by day-7 (Figure 5E). While there was a stepwise and drastic increase in MIF protein expression in KO^{WT} mice, in keeping with leukocyte infiltration following MI, the absolute levels were lower relative to WT or WT^{KO} mice (Figure 5E).

Somatic-cell MIF deficiency (KO^{WT}) promoted M1, but attenuated M2 macrophage marker genes post-MI

M1 macrophages are considered pro-inflammatory post-MI whereas M2 macrophages facilitate the healing process [32]. We investigated the impact of MIF derived from different cellular sources on macrophage polarisation following MI. Studies using qPCR revealed that cardiac expression of M1 macrophage markers, IL-1β, IFN-γ, TNFα and IL-6 was markedly increased at 3 and 7 days post-MI in all 3 groups. Whilst expression had declined at day-7 from day-3 levels in WT mice, expression of M1 marker genes was either increased or maintained at day-7 in both chimeric groups (Figure 6A). These changes are consistent with peak leukocyte infiltration at day-7 in both chimeric genotypes, particularly in KO^{WT} mice (Figure 5C). For M2 macrophage markers, TGFβ1, Arg-1 and MRC-1 were all increased at both days 3 and 7 after MI whilst CD163 expression was decreased in all 3 groups. Notably, cardiac expression of all M2 macrophage markers in KO^{WT} mice was significantly lower than that of WT or WT^{KO} mice at day 7 (Figure 6B), suggesting that poor post-infarct healing is partly attributable to impaired M2 activation as a consequence of cardiac MIF deficiency (Table 2).

Discussion

Using global MIFKO mice or chimeric mice with deficiency of MIF either in cardiac and non-leukocyte tissues, or in bone marrow derived cells, we examined the role of MIF in inflammation, wound healing and cardiac remodelling following MI. First, we observed that global MIF deletion protected against post-MI cardiac rupture and adverse cardiac remodelling. This effect of MIF deficiency was associated with suppressed cardiac inflammatory responses, evidenced by attenuation of leukocyte infiltration, expression of pro-inflammatory molecules and activity of MMP-9 and MMP-2. Second, we observed that MIF is a potent facilitator of the recruitment of macrophages to the site of injury, via mechanisms which depend upon the activation of p38 MAPK and NF-κB. Third, deficiency of MIF in leukocytes lowered risk of post-infarct cardiac rupture, reduced extent of post-infarct LV dilatation and dysfunction, and attenuated inflammatory responses, phenotypes similar to that seen in global MIFKO mice. In contrast, KO^{WT} mice with deficiency of MIF in the heart (and other non-leukocyte tissues) but expressing MIF in leukocytes, had a higher incidence of cardiac rupture and delayed healing associated with delayed leukocyte infiltration and enhanced M1 but impaired M2 macrophage marker expression. These results suggest distinct roles of cardiac and leukocyte MIF in regulating post-MI inflammation, healing and cardiac remodelling.

Although a number of experimental studies, including ours, have investigated the influence of MIF in ischemic heart injury [13-17], no previous study has defined the role of MIF in post-infarct healing and cardiac remodelling. Coronary artery occlusion in mice results in severe ischemic injury, strong inflammatory responses and cardiac remodelling, which mimic the clinical scenario of MI in humans. Using this model, we demonstrated that global MIF deletion protected the heart from acute wall rupture during the first week post MI. Further, echocardiography showed that by 4 weeks after MI, global MIFKO mice had smaller LV dimensions and preserved contractile function, confirming a detrimental role of MIF in post-infarct pathophysiology.

The inflammatory response following MI is critical for the removal of cellular debris and for fibrotic healing [6, 33]. However, excessive inflammatory responses and subsequent ECM degradation due to activation of MMPs, particularly MMP-9 and MMP-2, contribute to acute LV rupture and chronic chamber dilatation [34-36]. When compared to WT counterparts, global MIFKO mice had a lower risk of cardiac rupture and less severe LV dilatation and dysfunction. This was associated with reduced myocardial leukocyte infiltration, and suppressed expression of chemokines, pro-inflammatory cytokines and adhesion molecules, whereas expression of the anti-inflammatory cytokine, IL-10, was upregulated in MIFKO mice. These contributions of MIF to post-MI inflammation are similar to that we previously reported in the setting of prolonged cardiac ischemia-reperfusion [17]. MIF has been shown to upregulate MMP-9 expression in osteoblasts to promote bone resorption [37] and in macrophages to destabilize atherosclerotic plaques [38]. Our current study revealed that global MIF deletion attenuated expression and activity of MMP-9 and MMP-2 in the heart following MI. In keeping with these findings, our recent study demonstrated that inhibitory interventions using an anti-MIF monoclonal antibody or a small molecule inhibitor of MIF *ex vivo* attenuated the expression of MIF, MMP-9 and IL-6 by cultured peripheral blood mononuclear cells from human MI patients [39].

Macrophages from WT mice displayed significantly decreased chemotaxis in response to MIFKO infarct tissue, suggesting the importance of MIF located in the infarct myocardium in the recruitment of inflammatory cells. Similarly, MIFKO macrophages exhibited reduced capability of migration, indicating that both myocardial and leukocyte sources of MIF contribute to regional infiltration of immune cells following MI. This finding is congruent with recent reports showing that MIF increases leukocyte–endothelial interactions in human endothelial cells via promoting expression of adhesion molecules [40], and that MIF possesses chemokine-like function acting as a major regulator of inflammatory cell recruitment and atherogenesis [18]. It is also consistent with

two recent reports showing that MIF facilitates chemokine- or inflammation-induced migration of macrophages and neutrophils [41, 42].

p38 and JNK are major MAPK family members and play a vital role in myocardial injury through promoting cardiomyocyte apoptosis and inflammation [31, 43, 44]. The MAPK pathways and the NF-κB signal transduction cascade, are activated by cellular stress signals, such as inflammatory cytokines. MIF has been reported to activate p38 MAPK in rheumatoid arthritis [44] and colitis [45] or JNK in T lymphocytes and fibroblasts [46], and has been shown to enhance NF-κB activation in endothelial cells [40]. We therefore investigated the potential involvement of p38 MAPK and JNK as well as NF-κB signalling in MIF-mediated inflammatory action. We observed that global MIFKO hearts had reduced phosphorylation of both p38 MAPK and JNK. Interestingly, in the *in vitro* trans-well migration assays, migration of WT macrophages in response to exogenous MIF was abrogated by pre-treatment of macrophages with inhibitors of p38 MAPK or NF-κB, suggesting that these intracellular pathways are essential for MIF-mediated macrophage migration.

Previous studies reported protection of MIF against myocardial injury following a brief ischemia episode [13-16]. In the present study using MI model, as well as in our previous study using a prolonged ischemia/reperfusion model [17], we demonstrated a detrimental effect of MIF in MI via promotion of inflammatory responses and subsequent cardiac remodelling. As MIF is expressed in a variety of cell types including inflammatory cells [18] and cardiomyocytes [19], it is important to know whether MIF derived from different sources has different actions in these phenomena. We created chimeric mice with either somatic-cell (KO^{WT}) or bone-marrow derived-cell (WT^{KO}) MIF deficiency, to elucidate the contribution of MIF from these pools following MI. Compared to WT control mice, WT^{KO} mice were largely protected from post-MI cardiac rupture; in contrast, KO^{WT} mice had no protection against rupture, which was accompanied by more severe LV dilatation and dysfunction. Further, distinct temporal changes in leukocyte infiltration and MIF gene expression

after MI were also observed. Notably, the temporal change in MIF gene expression in the infarct myocardium of WT and KO^{WT} mice corresponded with the changes in leukocyte infiltration. WT mice had the highest leukocyte density and MIF gene expression in the infarct myocardium among the 3 groups. As leukocytes in WT^{KO} mice do not express MIF, such infiltration did not affect MIF mRNA levels post MI. In contrast, leukocytes in KO^{WT} mice express MIF thereby contributing to elevated MIF mRNA levels. Thus, infiltrated inflammatory cells are a predominant cellular source of MIF in the infarct myocardium of WT and KO^{WT} mice at the time points studied. While in WT^{KO} hearts, cardiac cells are the only cellular source of MIF. Interestingly, different from MIF at mRNA level, MIF protein content in both WT and WT^{KO} groups was decreased at day-3, relative to respective sham values, and restored at day-7 post MI. The reason for such dynamic changes may be due to release of cardiac MIF, in a large quantity, upon severe ischemic insult [47] albeit MIF gene transcription had already been upregulated. By day-7, upregulated MIF gene expression from various cells restored tissue MIF content, a similar phenomenon as previously reported [48]. Whereas, in KO^{WT} hearts, infiltrated leukocytes are the only source of MIF post MI, a steady increase in MIF protein level was associated with gradually increased leukocyte infiltration. Thus, deletion of MIF from immune cells (WT^{KO}) diminished MIF expression in the infarct myocardium, consistent with reduced inflammatory infiltration, cardiac rupture risk and attenuated adverse remodelling. Whereas, deficiency of MIF in somatic-cells or in the heart (KO^{WT}) resulted in delayed inflammatory response and extended the time window for rupture occurrence.

Macrophage polarisation results in dual actions of macrophages in inflammation and healing. Classically activated macrophages (M1) are recruited quickly into the damaged myocardium mediating further production of an array of pro-inflammatory mediators and cellular infiltrates [49, 50]. In contrast, alternatively activated macrophages (M2) accumulate later in the injured site, acting to terminate inflammation and promote synthesis of growth factors for angiogenesis and fibrotic healing [51, 52]. Compared to WT^{KO} counterparts, KO^{WT} mice displayed poor wound

healing evidenced by increased necrotic area, greater infarct wall thickness, and decreased collagen deposition or capillary density at day-7 and day-14 post-MI, implying an essential role of cardiac MIF in post-infarct healing. Moreover, KO^{WT} mice but not WT^{KO} mice exhibited diminished activation of M2 macrophages indicated by down-regulated expression of M2 macrophage markers. These findings were in keeping with greater leukocyte infiltration, higher risk of rupture and adverse cardiac remodelling and dysfunction in KO^{WT} versus WT^{KO} mice. However, although global MIFKO mice had moderately delayed healing indicated by a lower collagen deposition and thicker infarct wall versus WT mice at day-14, there was no difference in all healing parameters studied at 7 days and in necrosis absorption at 14 days between MIFKO and WT mice. Further, collagen deposition and gene expression of TGFβ, α-SMA by cultured cardiac fibroblasts isolated from the infarct tissue at day-4 post MI were similar between MIFKO and WT mice though collagen-1 mRNA level were higher in MIFKO fibroblasts. These observations suggest that MIF had a modest influence on the early healing process. It is worthwhile to point out that incidence of cardiac rupture follows the order of WT > KO^{WT} > global MIFKO ≥ WT^{KO} mice. WT^{KO} mice showed a trend to a lower rupture risk compared to global MIF deficiency, possibly due to a loss of protective endogenous cardiac MIF in the latter. Collectively, results from chimeric studies indicate that intrinsic cardiac MIF facilitates healing while inflammatory cell-derived MIF is detrimental to the heart following MI. These different effects may also partly explain the discrepancy between the findings of studies on the effects of MIF on ischemia-related events depending on the timing of observation, as cardiac healing effects and inflammatory effects, while coupled, are not simultaneous.

In conclusion, global MIF deletion attenuates MI-induced inflammatory responses thereby protecting the heart from cardiac rupture and adverse remodelling. Leukocyte-derived MIF promotes inflammatory infiltration, whereas cardiac-derived MIF affects healing although such influence on early healing process is minimal. The distinction between the contribution of cardiac,

compared to leukocyte, MIF, may be important in considering anti-MIF therapeutic interventions, which would be likely to target both leukocyte and non-leukocyte MIF.

Sources of Funding

This work was supported by grants (ID 472628, ID 1004235) from the National Health and Medical Research Council (NHMRC) of Australia and the Victorian Government's Operational Infrastructure Support Program. D.W. was a recipient of Australian National Heart Foundation PhD Scholarship (PB 10M 5481). A.M.D. and X.J.D. were NHMRC research fellows.

Disclosures

None.

References

[1] Roger VL, Go AS, Lloyd-Jones DM, Benjamin EJ, Berry JD, Borden WB, et al. Executive summary: heart disease and stroke statistics--2012 update: a report from the American Heart Association. Circulation 2012;125:188-97.

[2] Opie LH, Commerford PJ, Gersh BJ, Pfeffer MA. Controversies in ventricular remodelling. Lancet 2006;367:356-67.

[3] Pfeffer MA, Braunwald E. Ventricular remodeling after myocardial infarction. Experimental observations and clinical implications. Circulation 1990;81:1161-72.

[4] Frantz S, Bauersachs J, Ertl G. Post-infarct remodelling: contribution of wound healing and inflammation. Cardiovasc Res 2009;81:474-81.

[5] Dobaczewski M, Gonzalez-Quesada C, Frangogiannis NG. The extracellular matrix as a modulator of the inflammatory and reparative response following myocardial infarction. J Mol Cell Cardiol 2010;48:504-11.

[6] Frangogiannis NG, Smith CW, Entman ML. The inflammatory response in myocardial infarction. Cardiovasc Res 2002;53:31-47.

[7] Konstam MA, Kramer DG, Patel AR, Maron MS, Udelson JE. Left ventricular remodeling in heart failure: current concepts in clinical significance and assessment. JACC Cardiovasc Imaging 2011;4:98-108.

[8] Calandra T, Roger T. Macrophage migration inhibitory factor: a regulator of innate immunity. Nat Rev Immunol 2003;3:791-800.

[9] Morand EF, Leech M, Bernhagen J. MIF: a new cytokine link between rheumatoid arthritis and atherosclerosis. Nat Rev Drug Discov 2006;5:399-410.

[10] Calandra T, Echtenacher B, Roy DL, Pugin J, Metz CN, Hultner L, et al. Protection from septic shock by neutralization of macrophage migration inhibitory factor. Nat Med 2000;6:164-70.

[11] Morand EF, Bucala R, Leech M. Macrophage migration inhibitory factor: an emerging therapeutic target in rheumatoid arthritis. Arthritis Rheum 2003;48:291-9.

[12] Roger T, David J, Glauser MP, Calandra T. MIF regulates innate immune responses through modulation of Toll-like receptor 4. Nature 2001;414:920-4.

[13] Ma H, Wang J, Thomas DP, Tong C, Leng L, Wang W, et al. Impaired macrophage migration inhibitory factor-AMP-activated protein kinase activation and ischemic recovery in the senescent heart. Circulation 2010;122:282-92.

[14] Miller EJ, Li J, Leng L, McDonald C, Atsumi T, Bucala R, et al. Macrophage migration inhibitory factor stimulates AMP-activated protein kinase in the ischaemic heart. Nature 2008;451:578-82.

[15] Qi D, Hu X, Wu X, Merk M, Leng L, Bucala R, et al. Cardiac macrophage migration inhibitory factor inhibits JNK pathway activation and injury during ischemia/reperfusion. J Clin Invest 2009;119:3807-16.

[16] Koga K, Kenessey A, Powell SR, Sison CP, Miller EJ, Ojamaa K. Macrophage migration inhibitory factor provides cardioprotection during ischemia/reperfusion by reducing oxidative stress. Antioxid Redox Signal 2011;14:1191-202.

[17] Gao XM, Liu Y, White D, Su Y, Drew BG, Bruce CR, et al. Deletion of macrophage migration inhibitory factor protects the heart from severe ischemia-reperfusion injury: a predominant role of anti-inflammation. J Mol Cell Cardiol 2011;50:991-9.

[18] Bernhagen J, Krohn R, Lue H, Gregory JL, Zernecke A, Koenen RR, et al. MIF is a noncognate ligand of CXC chemokine receptors in inflammatory and atherogenic cell recruitment. Nat Med 2007;13:587-96.

[19] Takahashi M, Nishihira J, Shimpo M, Mizue Y, Ueno S, Mano H, et al. Macrophage migration inhibitory factor as a redox-sensitive cytokine in cardiac myocytes. Cardiovasc Res 2001;52:438-45.

[20] Fingerle-Rowson G, Petrenko O, Metz CN, Forsthuber TG, Mitchell R, Huss R, et al. The p53-dependent effects of macrophage migration inhibitory factor revealed by gene targeting. Proc Natl Acad Sci U S A 2003;100:9354-9.

[21] Gao XM, Dilley RJ, Samuel CS, Percy E, Fullerton MJ, Dart AM, et al. Lower risk of postinfarct rupture in mouse heart overexpressing beta 2-adrenergic receptors: importance of collagen content. J Cardiovasc Pharmacol 2002;40:632-40.

[22] Gao XM, Xu Q, Kiriazis H, Dart AM, Du XJ. Mouse model of post-infarct ventricular rupture: time course, strain- and gender-dependency, tensile strength, and histopathology. Cardiovasc Res 2005;65:469-77.

[23] Gao XM, Dart AM, Dewar E, Jennings G, Du XJ. Serial echocardiographic assessment of left ventricular dimensions and function after myocardial infarction in mice. Cardiovasc Res 2000;45:330-8.

[24] Fang L, Gao XM, Moore XL, Kiriazis H, Su Y, Ming Z, et al. Differences in inflammation, MMP activation and collagen damage account for gender difference in murine cardiac rupture following myocardial infarction. J Mol Cell Cardiol 2007;43:535-44.

[25] Gao XM, Wong G, Wang B, Kiriazis H, Moore XL, Su YD, et al. Inhibition of mTOR reduces chronic pressure-overload cardiac hypertrophy and fibrosis. J Hypertens 2006;24:1663-70.

[26] Ma Y, Halade GV, Zhang J, Ramirez TA, Levin D, Voorhees A, et al. Matrix metalloproteinase-28 deletion exacerbates cardiac dysfunction and rupture after myocardial infarction in mice by inhibiting M2 macrophage activation. Circ Res 2013;112:675-88.

[27] Gao XM, Ming Z, Su Y, Fang L, Kiriazis H, Xu Q, et al. Infarct size and post-infarct inflammation determine the risk of cardiac rupture in mice. Int J Cardiol 2010;143:20-8.

[28] Webb CS, Bonnema DD, Ahmed SH, Leonardi AH, McClure CD, Clark LL, et al. Specific temporal profile of matrix metalloproteinase release occurs in patients after myocardial infarction: relation to left ventricular remodeling. Circulation 2006;114:1020-7.

[29] Chen LL, Zhu TB, Yin H, Huang J, Wang LS, Cao KJ, et al. Inhibition of MAPK signaling by eNOS gene transfer improves ventricular remodeling after myocardial infarction through reduction of inflammation. Mol Biol Rep 2010;37:3067-72.

[30] Chi H, Barry SP, Roth RJ, Wu JJ, Jones EA, Bennett AM, et al. Dynamic regulation of pro- and anti-inflammatory cytokines by MAPK phosphatase 1 (MKP-1) in innate immune responses. Proc Natl Acad Sci U S A 2006;103:2274-9.

[31] Kyriakis JM, Avruch J. Sounding the alarm: protein kinase cascades activated by stress and inflammation. The Journal of biological chemistry 1996;271:24313-6.

[32] Gordon S, Taylor PR. Monocyte and macrophage heterogeneity. Nat Rev Immunol 2005;5:953-64.

[33] Frangogiannis NG. The immune system and cardiac repair. Pharmacol Res 2008;58:88-111.

[34] Heymans S, Luttun A, Nuyens D, Theilmeier G, Creemers E, Moons L, et al. Inhibition of plasminogen activators or matrix metalloproteinases prevents cardiac rupture but impairs therapeutic angiogenesis and causes cardiac failure. Nat Med 1999;5:1135-42.

[35] Matsumura S, Iwanaga S, Mochizuki S, Okamoto H, Ogawa S, Okada Y. Targeted deletion or pharmacological inhibition of MMP-2 prevents cardiac rupture after myocardial infarction in mice. J Clin Invest 2005;115:599-609.

[36] Sun M, Dawood F, Wen WH, Chen M, Dixon I, Kirshenbaum LA, et al. Excessive tumor necrosis factor activation after infarction contributes to susceptibility of myocardial rupture and left ventricular dysfunction. Circulation 2004;110:3221-8.

[37] Onodera S, Nishihira J, Iwabuchi K, Koyama Y, Yoshida K, Tanaka S, et al. Macrophage migration inhibitory factor up-regulates matrix metalloproteinase-9 and -13 in rat osteoblasts. Relevance to intracellular signaling pathways. The Journal of biological chemistry 2002;277:7865-74.

[38] Kong YZ, Yu X, Tang JJ, Ouyang X, Huang XR, Fingerle-Rowson G, et al. Macrophage migration inhibitory factor induces MMP-9 expression: implications for destabilization of human atherosclerotic plaques. Atherosclerosis 2005;178:207-15.

[39] White DA, Fang L, Chan W, Morand EF, Kiriazis H, Duffy SJ, et al. Pro-Inflammatory Action of MIF in Acute Myocardial Infarction via Activation of Peripheral Blood Mononuclear Cells. PLoS One 2013;8:e76206.

[40] Cheng Q, McKeown SJ, Santos L, Santiago FS, Khachigian LM, Morand EF, et al. Macrophage migration inhibitory factor increases leukocyte-endothelial interactions in human endothelial cells via promotion of expression of adhesion molecules. J Immunol 2010;185:1238-47.

[41] Fan H, Hall P, Santos LL, Gregory JL, Fingerle-Rowson G, Bucala R, et al. Macrophage migration inhibitory factor and CD74 regulate macrophage chemotactic responses via MAPK and Rho GTPase. J Immunol 2011;186:4915-24.

[42] Santos LL, Fan H, Hall P, Ngo D, Mackay CR, Fingerle-Rowson G, et al. Macrophage migration inhibitory factor regulates neutrophil chemotactic responses in inflammatory arthritis in mice. Arthritis Rheum 2011;63:960-70.

[43] Ma XL, Kumar S, Gao F, Louden CS, Lopez BL, Christopher TA, et al. Inhibition of p38 mitogen-activated protein kinase decreases cardiomyocyte apoptosis and improves cardiac function after myocardial ischemia and reperfusion. Circulation 1999;99:1685-91.

[44] Santos LL, Lacey D, Yang Y, Leech M, Morand EF. Activation of synovial cell p38 MAP kinase by macrophage migration inhibitory factor. J Rheumatol 2004;31:1038-43.

[45] Ishiguro Y, Ohkawara T, Sakuraba H, Yamagata K, Hiraga H, Yamaguchi S, et al. Macrophage migration inhibitory factor has a proinflammatory activity via the p38 pathway in glucocorticoid-resistant ulcerative colitis. Clin Immunol 2006;120:335-41.

[46] Lue H, Dewor M, Leng L, Bucala R, Bernhagen J. Activation of the JNK signalling pathway by macrophage migration inhibitory factor (MIF) and dependence on CXCR4 and CD74. Cell Signal 2011;23:135-44.

[47] Chan W, White DA, Wang XY, Bai RF, Liu Y, Yu HY, et al. Macrophage migration inhibitory factor for the early prediction of infarct size. J Am Heart Assoc 2013;2:e000226.

[48] Yu CM, Lai KW, Chen YX, Huang XR, Lan HY. Expression of macrophage migration inhibitory factor in acute ischemic myocardial injury. J Histochem Cytochem 2003;51:625-31.

[49] Gordon S. Alternative activation of macrophages. Nat Rev Immunol 2003;3:23-35.

[50] Ma J, Chen T, Mandelin J, Ceponis A, Miller NE, Hukkanen M, et al. Regulation of macrophage activation. Cell Mol Life Sci 2003;60:2334-46.

[51] Odegaard JI, Chawla A. Alternative macrophage activation and metabolism. Annu Rev Pathol 2011;6:275-97.

[52] Benoit M, Desnues B, Mege JL. Macrophage polarization in bacterial infections. J Immunol 2008;181:3733-9.

Table 1. Echocardiographic parameters of wild type and chimeric mice (WT^{KO} and KO^{WT}) following myocardial infarction

	Day-0			Day-7			Day-14s		
	WT	WT^{KO}	KO^{WT}	WT	WT^{KO}	KO^{WT}	WT	WT^{KO}	KO^{WT}
	n=25	n=21	n=26	n=13	n=15	n=18	n=13	n=15	n=11
HR (bpm)	598±13	604±11	582±13	600±10	588±17	593±34	590±15	610±10	613±11
LVEDd (mm)	3.77±0.06	3.65±0.04	3.50±0.07	4.58±0.17*	4.45±0.16*	4.89±0.28*	5.03±0.22*	4.65±0.31*	5.34±0.31*†‡
LVESd (mm)	2.50±0.05	2.35±0.05	2.28±0.07	3.45±0.14*	3.28±0.18*	3.86±0.31*†‡	4.21±0.22*	3.82±0.14*	4.40±0.34*‡
PWd (mm)	0.80±0.01	0.83±0.03	0.82±0.02	0.80±0.03	0.84±0.02	0.79±0.05	0.76±0.03	0.77±0.04	0.88±0.03
PWs (mm)	1.24±0.03	1.28±0.03	1.29±0.03	1.03±0.04*	1.13±0.04*	1.02±0.08*	0.98±0.05*	1.11±0.04*	0.94±0.06*
FS (%)	33.6±1.4	35.6±1.2	34.8±1.6	24.6±1.7*	26.3±1.8*	21.1±1.7*†‡	16.3±1.6*	18.0±1.1*	13.6±0.9*†‡

Values are mean ± SEM, **P<0.05* vs. baseline, *†P<0.05* vs. WT at the same time point. *‡P<0.05* vs. WT^{KO} at the same time point. WT, wild type; WT^{KO}, bone marrow cell/leukocyte-MIF deficient mice; KO^{WT}, somatic cell/heart-MIF deficient mice; HR, heart rate; LVEDd, left ventricular end-diastolic diameter; LVESd, LV end-systolic diameter; PWd, LV posterior wall thickness at diastole; PWs, LV posterior wall thickness at systole; FS, fractional shortening.

Table 2. Histological analysis of post-infarct healing in hearts of WT and chimeric mice (WT^{KO}, KO^{WT}).

	Day-7 MI			Day-14 MI		
	WT (n=7-8)	WT^{KO} (n=6-8)	KO^{WT} (n=7)	WT (n=7-8)	WT^{KO} (n=7)	KO^{WT} (n=7-8)
Infarct Size (%)	29.6±3.2	29.3±3.4	31.5±3.7	34.6±2.4	34.6±3.3	34.5±2.6
Residual necrotic area (% infarct area)	17.8±5.7	18.9±3.6	30.4±2.2†‡	2.6±0.8*	4.3±1.6*	4.9±0.9*
Infarct wall thickness (μm)	600±46	492±66	559±78	316±31*	245±13*†	344±40*‡
Collagen deposition (% of infarct area)	24.0±8.0	3.8±0.5†	3.7±0.9†	59.0±2.0*	43.7±1.8*†	38.3±1.4*†‡
Capillary density (vessels No./mm^2)	1689±237	1906±188	1766±175	1881±123	2301±201*†	1812±112‡

Values are mean ± SEM, **P<0.05* vs. respective values at day-7 MI, †*P<0.05* vs. WT at same time point, ‡*P<0.05* vs. WT^{KO} at the same time point. WT, Wild Type; WT^{KO}, bone marrow cell/leukocyte-MIF deficient mice; KO^{WT}, somatic cell/heart-MIF deficient mice; MI, myocardial infarction.

Figure legends

Figure 1. Global MIF deletion (MIFKO) reduced incidence of cardiac rupture and alleviated cardiac remodelling and dysfunction following myocardial infarction (MI). A, Kaplan-Meier survival analysis of wild type (WT) and MIFKO mice up to 4 weeks following MI, all sham operated animals survived (not shown). n=49 for WT and 29 for MIFKO group. **B,** Cumulative incidence of cardiac rupture leading to mortality in WT and MIFKO mice. Numbers represent the group size. **C**, Quantitative analysis of infarct size at autopsy in those mice dying of rupture within 3-5 days (acute phase) and in surviving mice at 4 weeks post MI (chronic phase). Numbers in the bar represent the group size. **D,** Echocardiographic data showing that left ventricular end-diastolic and end-systolic dimensions (LVEDd, LVESd) were smaller and fractional shortening (FS) was greater in MIFKO than in WT mice at 4 weeks after MI, indicating less severe LV remodelling and dysfunction in MIFKO mice. ***P<0.05* vs. WT, n=15-20 per time point.

Figure 2. Temporal changes in leukocyte infiltration and gene expression of cytokines, chemokine and adhesion molecules in global MIF deficient (MIFKO) and wild type (WT) mice following myocardial infarction (MI). A, Representative images of CD45 positive immunofluroescent staining for leukocytes in the infarct region at 3 days after MI. The purple colour indicates overlap of CD45 positive staining (red) with DAPI (blue) staining for nuclei. Bar=100 μm. **B,** Quantification of leukocytes (CD45 positive cells) in the infarct and border regions from different time points after MI. **C-G,** Changes in mRNA level of monocyte chemoattractant protein-1 (MCP-1), intracellular adhesion molecule 1 (ICAM-1), vascular cell adhesion molecule 1 (VCAM-1), interlukin-1β (IL-1β) and IL-10 in the

infarct tissue of WT and MIFKO mice at different time points after MI. **H,** Temporal change of IL-1β plasma level in WT and MIFKO mice with either sham-operated or MI. ***P<0.05* vs. respective sham, †*P<0.05* vs. WT at the same time point. n=4 per sham group, n=7-8 per MI group.

Figure 3. Global MIF deletion (MIFKO) attenuated activity and gene expression of matrix metallanoprotienase-9 (MMP-9) and MMP-2 following myocardial infarction (MI). A, Representative images of gelatine zymography demonstrating temporal changes of MMP-9 and MMP-2 activities in WT and MIFKO mice following MI. **B,** Quantitative analyses of active MMP-9 and MMP-2 by zymography in WT and MIFKO mice from sham-operated and infarcted tissues. n=3 for each sham group, n=5 for each MI group. **C,** temporal changes in mRNA levels of MMP-9 and MMP-2 from WT and MIFKO mice following MI. n=4 per sham group, n=7-8 per MI group. ***P<0.05* vs. sham, †*P<0.05* vs. WT at the same time point.

Figure 4. Phosphorylation of pro-inflammatory signalling kinases was reduced in global MIF deficient (MIFKO) mice and MIF promoted macrophage infiltration in the infarct myocardium. A, Representative immunoblotting images for phospho- and total-p38 mitogen-activation protein kinase (p/t-p38) and c-Jun N-terminal kinase (p/t-JNK) in hearts of sham-operated (SH) or infarct wild type (WT) and MIFKO mice. **B,** Quantitative analysis of p/t-p38 MAPK and p/t-JNK in WT and MIFKO mice. ***P<0.05 vs.* sham, †*P<0.05* vs. WT at day 3, n=3 per sham group, n=5 per MI group). **C,** Macrophage chemotaxis in response to sham or homogenised infarct tissue from WT or MIFKO mice at day 3. Cells/HPF, cells/high

power field. ***P<0.05* vs. other conditions. MCP-1 Ab, monocyte chemoattrant protein-1 neutralizing monoclonal antibody (eBioscience, 5 μg/ml). **D,** Chemotaxis by quantitative migration analysis of WT macrophage or pre-treated WT macrophages with inhibitors for p38 MAPK (p38i, SB203580, 10 μM) or NF-κB inhibitor (NF-κBi, Bay 11-7082, 2 μM) for 1 hr in response to recombinant MIF (rMIF, 40 ng/ml) in trans-well experiments. ***P<0.05*. Experiments were performed in triplicates.

Figure 5. Survival, incidence of cardiac rupture, cardiac expression of MIF and leukocytes infiltration in wild type (WT), global MIF deficient (KO) or chimeric mice with either bone marrow derived cell-MIF deficiency (WT^{KO}) or somatic cell-MIF deficiency (KO^{WT}) following myocardial infarction (MI). A, Kaplan-Meier survival analyses for WT, KO, WT^{KO} and KO^{WT} mice after MI. **B,** Cumulative incidence of cardiac rupture leading to mortality in WT, KO, WT^{KO} and KO^{WT} mice. Numbers represent group size. **C,** Time course of CD45 positive leukocyte densities in the infarct and border zones of WT, WT^{KO} and KO^{WT} mice following MI. **D,** Temporal change in MIF gene expression by qPCR in WT mice and both chimeric models following MI. ***P<0.05* vs. sham, $^{\#}P<0.05$. n=3 per sham group, n=5-8 per MI group. **E,** Temporal change in MIF protein expression in WT mice and both chimeric models following MI. ***P<0.05* vs. sham, †*P<0.05* vs. WT^{KO} at each time point. n=3 per sham group, n=5 per MI group.

Figure 6. Expression pattern of markers for M1 and M2 macrophages in wild type (WT) and chimeric mice with either bone marrow derived cell-MIF deficiency (WT^{KO}) or somatic cell-MIF deficiency (KO^{WT}) following myocardial infarction (MI). A, mRNA

expression of M1 macrophage markers, interleukin 1β (IL-1β), interferon-γ (IFN-γ), tumor necrosis factor α (TNFα) and IL-6 in WT, WT^{KO} and KO^{WT} mice. **B,** mRNA expression of M2 macrophage markers, transforming growth factor β1 (TGFβ1), arginase 1 (Arg-1), macrophage mannose receptor 1 (MRC-1) and CD163 in WT, WT^{KO} and KO^{WT} mice. Data expressed as fold change from WT sham expression. n=4 per sham group, n=6 per MI group. *****$P<0.05$ vs. sham, $^{\#}P<0.05$.

Figure

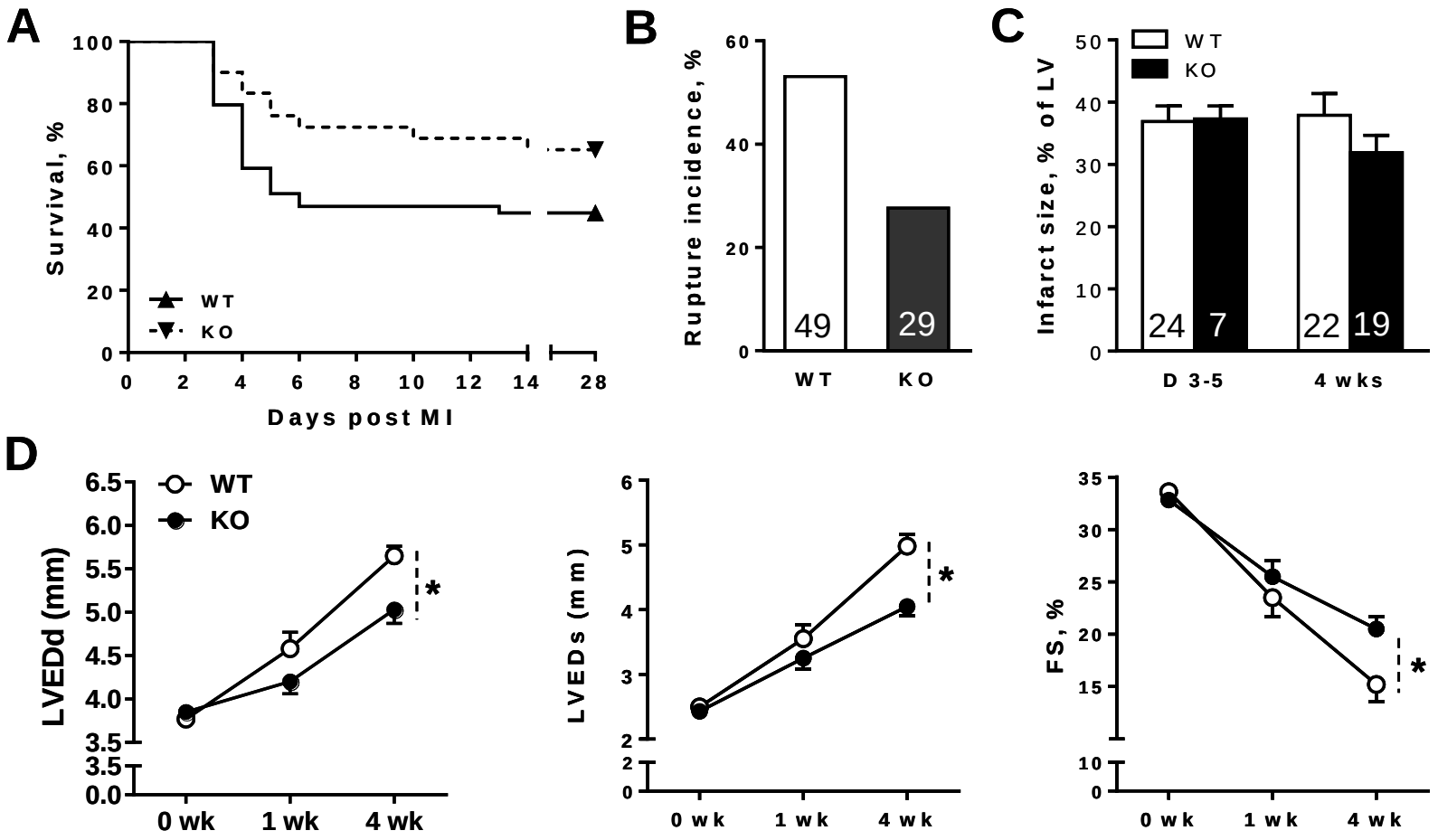

Figure 1

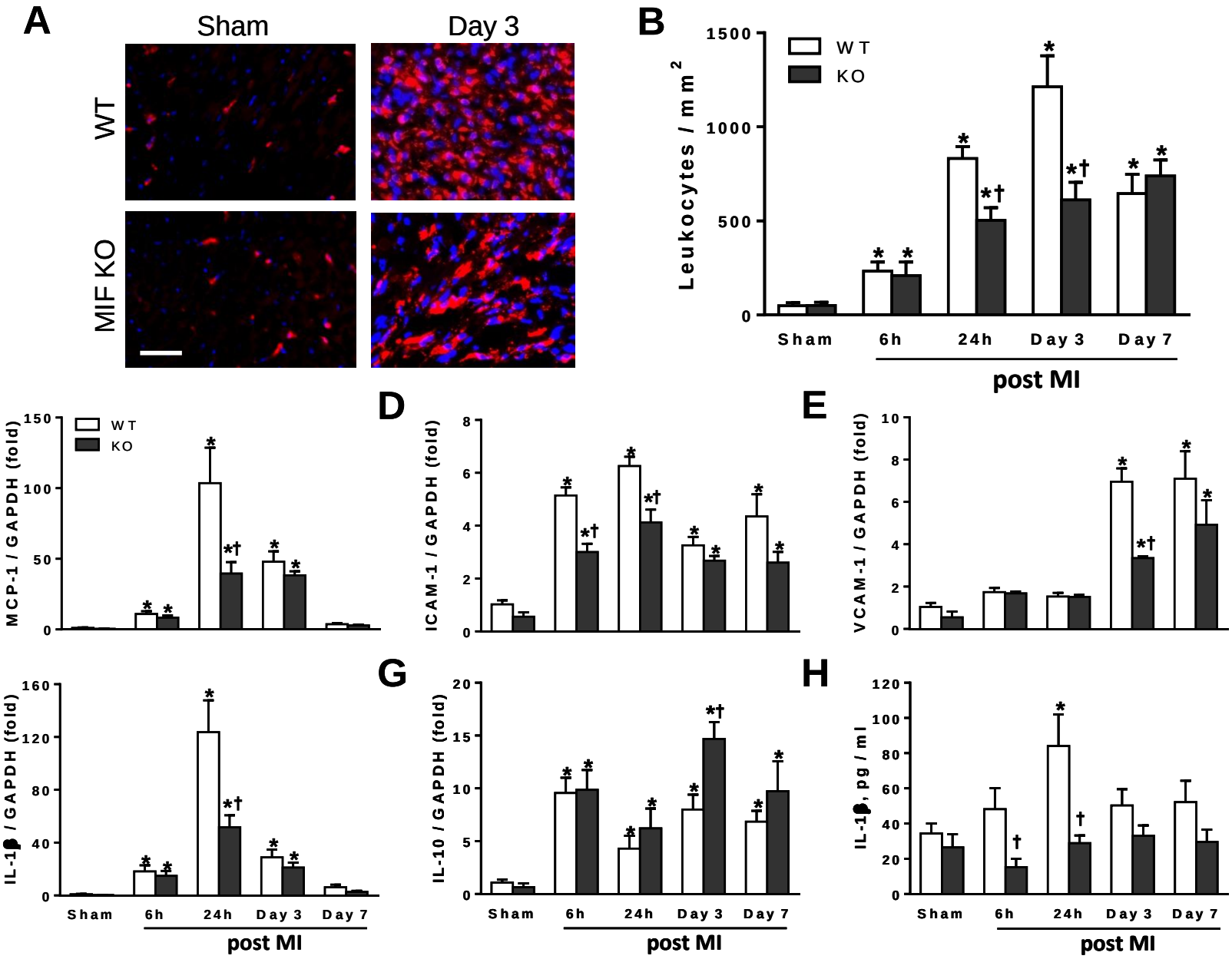
A
Sham
Day 3
WT
MIF KO
B
WT
KO
Leukocytes / mm²
1500
1000
500
0
Sham
6h
24h
Day 3
Day 7
post MI
C
MCP-1 / GAPDH (fold)
150
100
50
0
D
ICAM-1 / GAPDH (fold)
8
6
4
2
0
E
VCAM-1 / GAPDH (fold)
10
8
6
4
2
0
F
IL-1β / GAPDH (fold)
160
120
80
40
0
G
IL-10 / GAPDH (fold)
20
15
10
5
0
H
IL-1β, pg / ml
120
100
80
60
40
20
0

Figure 2

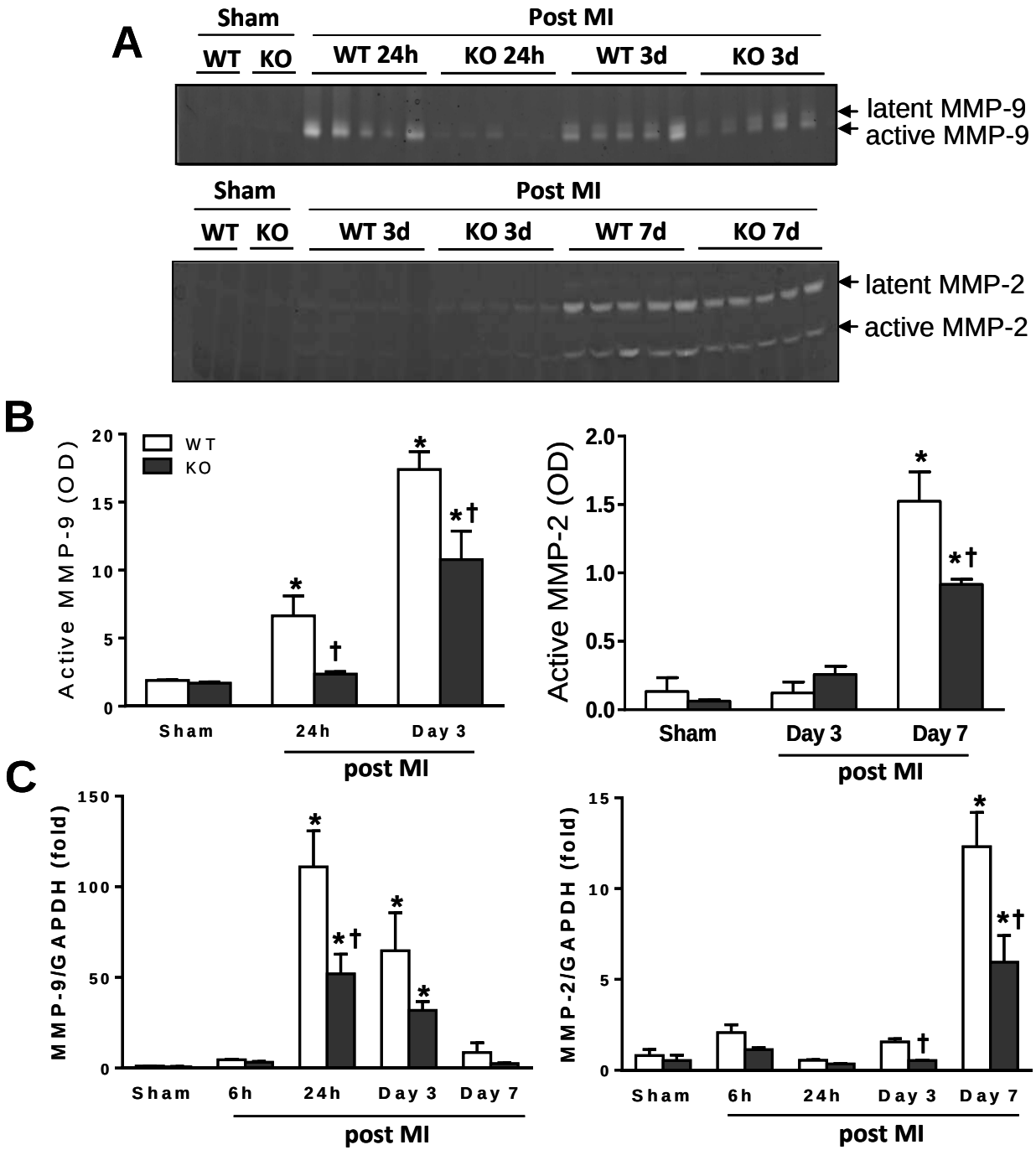
A
Sham
Post MI
WT
KO
WT 24h
KO 24h
WT 3d
KO 3d
latent MMP-9
active MMP-9
Sham
Post MI
WT
KO
WT 3d
KO 3d
WT 7d
KO 7d
latent MMP-2
active MMP-2
B
Active MMP-9 (OD)
WT
KO
Sham
24h
Day 3
post MI
Active MMP-2 (OD)
Sham
Day 3
Day 7
post MI
C
MMP-9/GAPDH (fold)
Sham
6h
24h
Day 3
Day 7
post MI
MMP-2/GAPDH (fold)
Sham
6h
24h
Day 3
Day 7
post MI

Figure 3

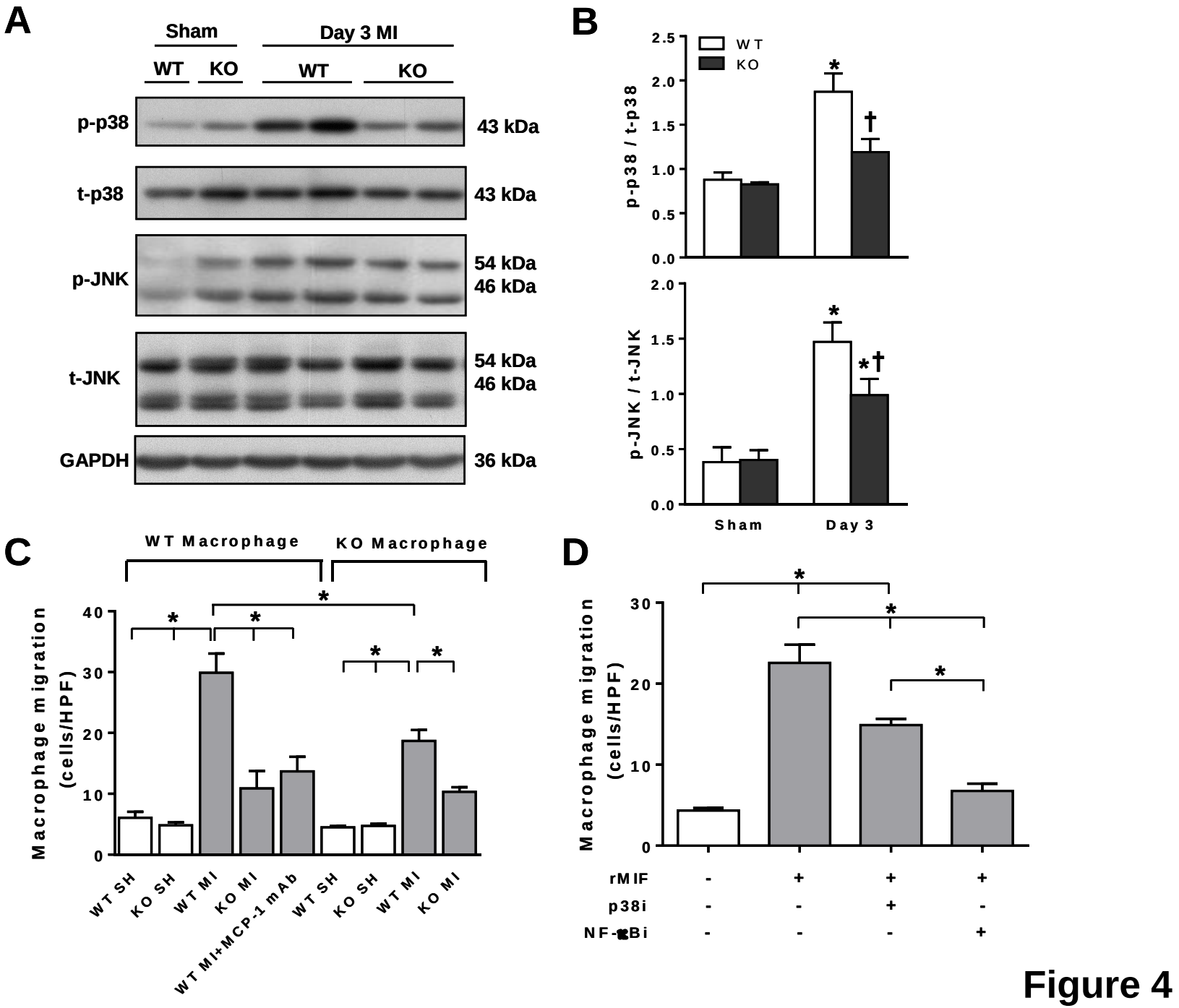
A
Sham
Day 3 MI
WT
KO
WT
KO
p-p38
43 kDa
t-p38
43 kDa
p-JNK
54 kDa
46 kDa
t-JNK
54 kDa
46 kDa
GAPDH
36 kDa
B
WT
KO
p-p38 / t-p38
p-JNK / t-JNK
Sham
Day 3
C
WT Macrophage
KO Macrophage
Macrophage migration (cells/HPF)
WT SH
KO SH
WT MI
KO MI
WT MI+MCP-1 mAb
D
Macrophage migration (cells/HPF)
rMIF
p38i
NF-κBi

Figure 4

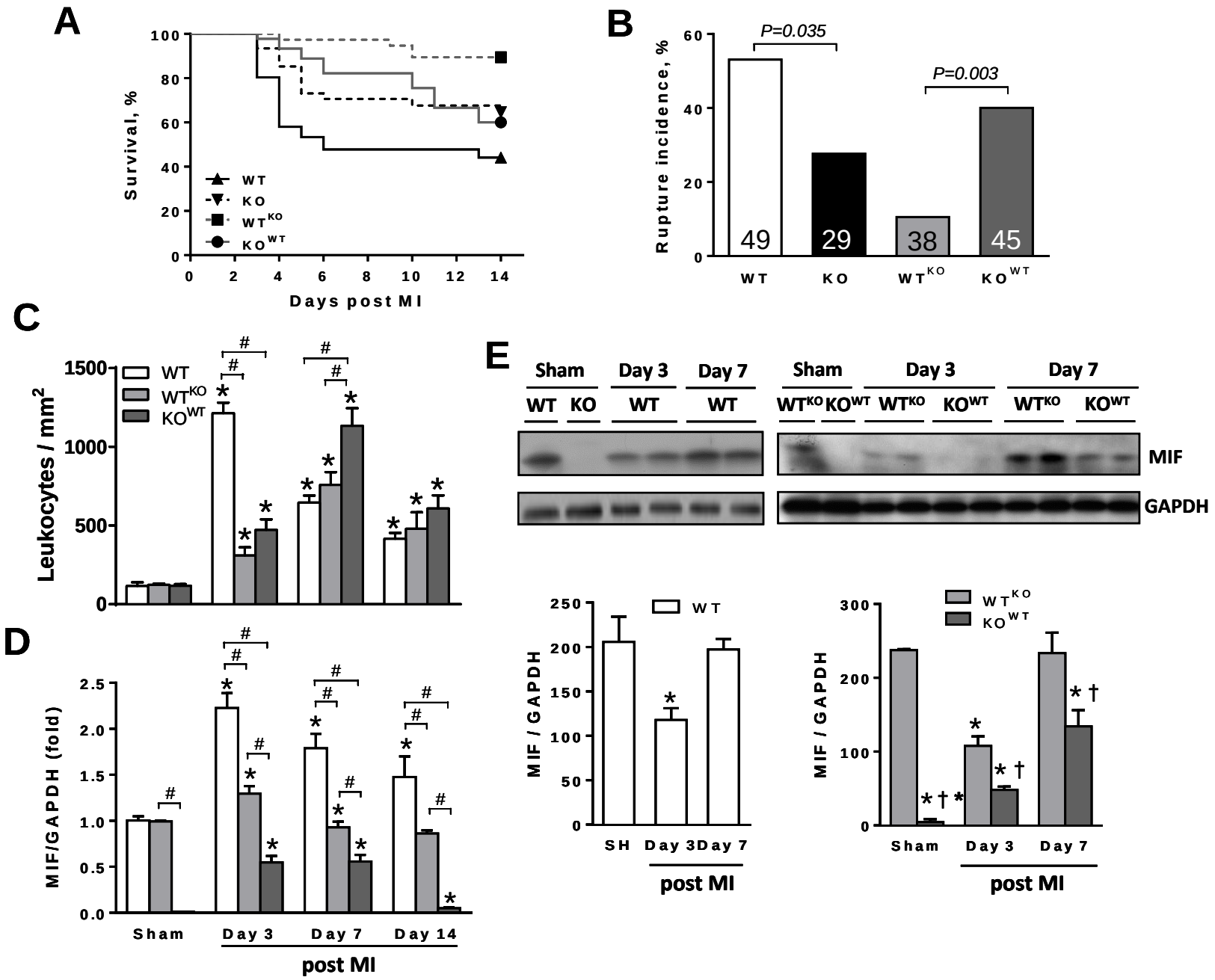
A
Survival, %
Days post MI
WT
KO
WT^KO
KO^WT
B
Rupture incidence, %
P=0.035
P=0.003
49
29
38
45
C
Leukocytes / mm2
D
MIF/GAPDH (fold)
Sham
Day 3
Day 7
Day 14
post MI
E
MIF
GAPDH
MIF / GAPDH
SH
post MI

Figure 5

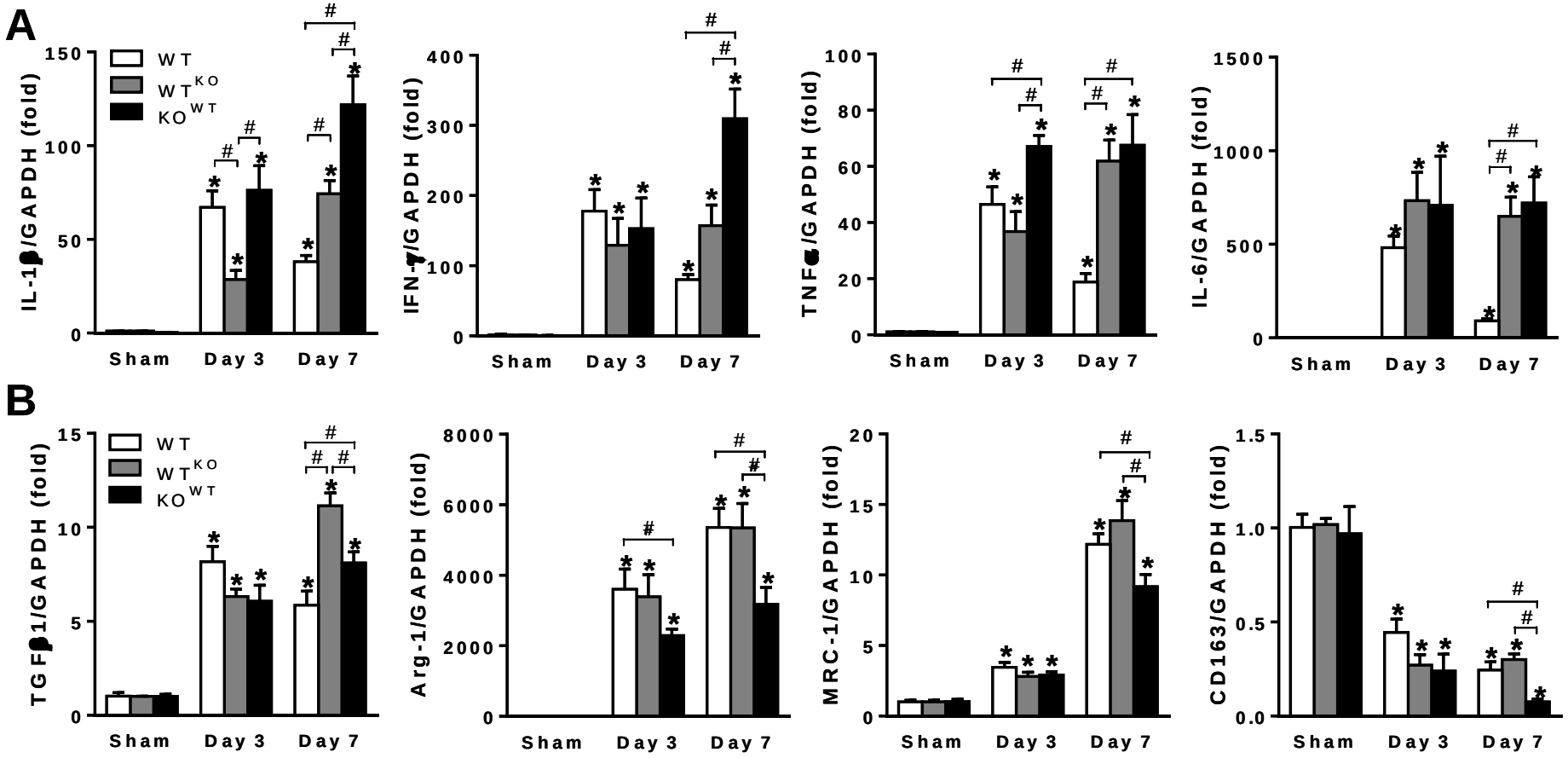
A
B
WT
WT^KO
KO^WT
IL-1β/GAPDH (fold)
IFN-γ/GAPDH (fold)
TNFα/GAPDH (fold)
IL-6/GAPDH (fold)
TGFβ1/GAPDH (fold)
Arg-1/GAPDH (fold)
MRC-1/GAPDH (fold)
CD163/GAPDH (fold)
Sham
Day 3
Day 7

Figure 6

JMCC7818-R2

Online Supplementary Material

Detailed Methods

Animals

All animal experiments were approved by AMREP Animal Ethic Committee complying with the "Australian Code of Practice for the Care and Use of Animals for Scientific Purposes (2011 edition)." Ten-week-old male global MIF deficient (MIFKO) mice and wild type (WT) littermates were used in this study [1].

Induction of MI

Briefly, animals were anesthetized using a mixture of ketamine, xylazine and atropine (100, 20 and 1.2 mg/kg, respectively, i.p.) and mechanically ventilated. Under a surgical microscope, left thoracotomy was performed to expose the heart. The left coronary artery was identified and ligated with a 7–0 silk suture at a level approximately 2 mm below the edge of the left auricle. Sham-operation was also performed without ligating the coronary artery [2, 3]. After surgery mice were monitored daily for 4 weeks and autopsy was performed on all mice found dead to identify the cause of death such as post-myocardial infarction (MI) cardiac rupture or heart failure, as described previously [2, 3]. Some mice were sacrificed at 6 and 24 h, 3, 7 and 14 days, and 4 weeks, respectively, following MI. Infarct and non-infarct myocardium were separated and snap frozen in liquid nitrogen and stored at -80°C for molecular assays. Further, some hearts were fixed in 10% formalin or fresh frozen for embedding with OCT for histological analyses.

Determination of Infarct Size

Infarct size was determined using the method of fractional left ventricle (LV) surface area as

previously described [3]. Briefly, the right ventricle and atria were removed and LV was cut open and pinned on a wax board. Digital images of the endocardial view of the LV were acquired. Infarct areas were easily identified by pale colour and clear demarcation from the non-infarct regions. Images were analysed using Image Pro Plus (Media Cybernetics Inc., USA). Infarct size was determined by dividing the infarct endocardial surface area over the entire LV area.

Echocardiography

Mice were anesthetized using a mixture of ketamine, xylazine and atropine (50, 10 and 1.2 mg/kg, respectively, i.p.). Using an iE33 ultrasound system and a 15MHz linear probe (Philips), a short-axis view of the LV close to papillary muscles was obtained. A 2D guided M-mode trace crossing the anterior and posterior wall of the LV was acquired. Images were analysed by a single investigator in a blinded fashion. LV dimensions at end-diastole and end-systole (LVEDd, LVESd), posterior wall thickness at diastole and at systole (PWd, PWs) were measured and fractional shortening (FS%) was calculated, as previously described [4, 5].

Immunofluorescence staining

Leukocyte staining. Briefly, fresh-frozen LV sections were incubated with rat anti-mouse CD45 antibody for leukocytes (1:50, BD Pharmingen) for 1 h followed by incubation with secondary antibody Alexa Fluor 546 goat anti-rat IgG (1:1000, Invitrogen) for 30 min. Nuclei were stained by nuclear acid dye, 4', 6-diamidino-2-phenylindole (DAPI) (Invitrogen, 1:1000). Overlayed images of CD45 positive stained cells with DAPI stained nucleus were identified as positive staining. Multiple images (8-10 per heart) covering the entire infarct region of the LV section were acquired digitally using Olympus BX61 fluorescence microscope and AnalySIS FIVE software (Olympus) at ×20 magnification and the number of inflammatory cells was counted manually in a blinded fashion, as previously described [5, 6].

Endothelial cell staining. In order to quantify capillary densities, formalin fixed LV sections were stained with Alexa Fluor® 568 isolectin GS-IB_4 conjugate (1:10 dilution, Invitrogen, Aust.) at 4°C overnight and then mounted with anti-fade mounting media. Images (4~5 per LV section) were acquired at ×20 magnification in the border zone of the infarct area using an Olympus BX61 fluorescence microscope and analysed using Image Pro Plus (Media Cybernetics Inc., USA) and expressed as number of capillaries per mm^2.

Quantitative real time-PCR

RNA was extracted from sham-operated and infarct myocardium using TRIzol reagent (Invitrogen, USA) according to the manufactures instructions. Total mRNA concentration was quantified using a Nanodrop ND-2000 spectrophotometer (Thermo Scientific). Reverse transcription of equal mRNA concentrates was achieved by M-MLV RT method according to manufacture's instructions (Invitrogen, 28025-23). Gene expression of monocyte chemotactic protein-1 (MCP-1), intercellular adhesion molecule-1 (ICAM-1), vascular cell adhesion molecule 1 (VCAM-1), interleukin-1β (IL-1β), IL-10, matrix metallanoprotienase-9 (MMP-9), MMP-2 and transforming growth factor β1 (TGFβ1) were assessed by quantitative real time PCR (qPCR, Applied Biosystems 7500 fast real-time PCR system) and normalised to housekeeping gene GAPDH, as previously described [5, 7].

Enzyme-linked immunosorbent assay

Enzyme-linked immunosorbent assay (ELISA) was performed in duplicates using a commercial mouse IL-1β (Life Research, Australia) ELISA kits, according to the manufacture's instructions.

Gelatin zymography

Gelatin zymography was performed on a 7.5% acrylamide, 0.5% gelatine SDS page as previously described [7]. Briefly, 200 μg of proteins was loaded with loading buffer for electrophoresis. The gel was washed, incubated for 16 h at 37°C, and stained by 0.1% Coomassie for 1 h then de-stained

until visible bands formed (3-4 h). The gel was scanned and bands quantified using Quantity One (Version 4.5.2, Bio-Rad Laboratories, USA).

Immunoblotting

Proteins were extracted from sham-operated and infarct myocardium and normalised using BCA protein quantification assay (Thermo Scientific, USA). Proteins were separated on a 10% SDS-PAGE and transferred to a PVDF membrane. The membrane was blocked with 5% skim milk in TBST and then incubated with primary antibodies including phospho- or total-p38 mitogen-activation protein kinase (p-p38 and t-p38 MAPK), p-JNK and t-JNK and GAPDH (all from Cell Signalling, MA, USA) and MIF (polyclonal antibody, Abcam, UK) overnight at 4°C followed by incubation with corresponding secondary antibody conjugated with horseradish peroxidise (Santa Cruz Technologies Biotechnologies, TX, USA). Exposure to x-ray film was achieved by enhanced chemiluminescence reagent (Millipore, USA). Films were scanned and band intensity quantified using Quantity One software (Version 4.5.2, Bio-Rad Laboratories, USA), as reported previously [5].

Histology

LV sections from formalin fixed tissue was stained for hemotoxylin and eosin (H&E) to assess remaining coagulative necrotic areas in the infarct region and infarcted LV wall thickness. Picosirius red straining was used to identify collagen density in the infarct area of the LV. Microscopic images were collected at ×4 magnification from H&E stained LV sections (2 sections per heart) for infarct wall thickness measurement and at ×10 magnification from H&E or Picosirius red strained LV sections (6 per heart) to cover entire infarct region for determining the coagulative necrotic area and collagen density using Image-Pro Plus 6.0 software (Media Cybernetics, Inc, USA). Ten measurements of infarct wall thickness cross the entire infarct segment were obtained

and averaged. Necrotic area and collagen positive stained area were calculated and expressed as percentage in the infarct area, as described previously [8, 9].

Cell culture experiments.

Hypoxic stimulation of cardiomyocytes (CM) and fibroblasts (CF).

Primary neonatal CM and CF were isolated from 1-day-old C57Bl/6 mouse pups. Briefly, pups were decapitated and hearts excised and washed in cold Hanks Balanced Salts Solution (HBSS). The ventricle was dissociated with trypsin (1 mg/ml) at 4°C overnight, then digested with collagenase/HBSS (~ 0.4 mg/heart) at 37°C for 10 min. Supernatant containing cells was collected into DMEM (Invitrogen) supplemented with 5% FBS. After centrifugation, the cell pellet was gently resuspended in DMEM/10% FBS with a mixture of anti-biotics/anti-mycotics (1%, Invitrogen) and incubated for 50 min at 37^{o}C. CF readily attached to the bottom of the culture dish and CM enriched cell suspension was collected and plated at a density of 0.35×10^{6} for 48 h with addition of 0.1 mM Bromodeoxyuridine (BrdU) to prevent non-myocyte proliferation and growth. Passage 2 CF were seeded at a density of 0.15×10^{6} overnight. Both CM and CF underwent serum starvation for 24 h followed by a media change with HEPES buffered solution containing (in mM) HEPES 4, NaCl 137, KCl 3.5, $MgSO_4$ 0.5, $CaCl_2$ 0.884, D-glucose 5.55, and 2% FBS (pH 7.4). Before hypoxia, cell images of CM and CF were taken using ×4 lens and cell counting performed with Image J software (NIH, USA) to ensure a similar cell density of ~450 cells/field was achieved. For hypoxia treatment, cultured dishes containing CM and CF were placed in a sealed modular incubation chamber (QNA International, East Ivanhoe) and flushed with 95%N_2/5% CO_2 gas for 15 min to deplete oxygen. The chamber was then sealed and placed into an incubator for 6 h. Control CM and CF remained under normoxia (5% CO_2 in air). Supernatant media were collected for MIF assay using ELISA (Rat MIF ELISA kit, ElAab Science Co. Wuhan, China) and normalized by cell density.

Adult mouse cardiac fibroblast isolation and culture.

We followed the protocol reported by Haudek et al with modifications [10]. Briefly, the infarct tissue of both adult global MIFKO (n=3) and WT mice (n=3) was collected at 4 days after MI and minced into small 2×2 mm pieces and digested in collagenase buffer containing Hanks solution, collagenase (1 mg/ml, CLS-2, Worthington) and 2.5% trypsin at 37°C for 10 min. Supernatant was removed and collagenase buffer was added to the remaining tissue fragments with repetition of these steps a few times to fully digest the tissue. All cell supernatant in 10% FBS/DMEM were combined and centrifuged, cell pellet was resuspended and incubated overnight. Non-adherent cells were removed and adherent cells cultured until reaching confluence. Passage 4 CF were used for the following experiments. (1) For cell proliferation: CF were seeded at a density of 5000 cell/cm^2 and incubated overnight then followed by starvation for 24 h. Then multiple cell images were taken at 0 and 48 h (incubation in 1% FBS/DMEM) time points to count the cell number using Image J software and expressed as cell number/cm^2. (2) For collagen deposition: CF were seeded at 1×10^4 cells/cm^2 and cultured in 10% FBS/DMEM for 24 h then followed by starvation for 24 h. Before and after 48 h incubation in 1% FBS/DMEM, the media was removed and wells were washed with PBS, then 200 µl of 0.1% picrosirius red dye was added into the well for 1 h incubation. After incubation, unbound dye was washed away and bound complex was dissolved in 200 µl of 0.5% sodium hydroxide and transferred to a 96 well plate. Collagen content was quantified by a spectrophotometry at 450 nm and collagen deposition was expressed as a percentage of baseline level (0 h time point). (3) Fibrosis-related gene expression: CF were seeded at 2×10^4 cells/cm^2 and cultured in 10% FBS/DMEM for 24 h then followed by starvation for 24 h. After 48 h incubation in 1% FBS/DMEM, cells were collected and TRIzol was added for RNA extraction. Expression of TGFβ, α-smooth muscle actin (α-SMA) and collagen-1 and -3 were assessed by qPCR and normalised to housekeeping gene β-actin, as described above.

Trans-well migration assay

Macrophages were collected from the peritoneal cavities of WT and global MIFKO mice 4 days following a peritoneal injection of 2 ml 2% thioglycollate (BD Bioscience). Cells were resuspended at a density of 2×10^5 cells/ml in DMEM after erythrocyte lysis. Migration assay was performed in a 24-well Transwell® 8 μm polycarbonate membrane plate (Corning Incorporated, NY, USA) according to the manufacturer's instructions. Cardiac tissues (sham and infarct) were homogenised and proteins quantified via Bradford protein assay and normalized to 50 mg/ml in DMEM. An aliquot of 500 μl was added to the bottom chamber. Further, WT infarct tissue homogenate (3 days after MI) was added to the lower chamber with or without a neutralising MCP-1 monoclonal antibody (5 μg/ml, eBioscience). Macrophages (1×10^5 in 500 μl) was added to the top chamber insert and incubated at 37°C for 3 h. After incubation, non-migrated macrophages were removed by washing with DMEM and wiping with a cotton swab. The top insert containing migrated macrophages was fixed in methanol/Acetic Acid (3:1) for 6 min followed by staining with 0.1% Crystal Violet in PBS with 2% ethanol for 1 h. Migrated macrophages were counted at five random high-power fields (×400) using a inverted light microscope (CYX-41 Olympus, Japan), The number was averaged and expressed as macrophages per high powered field. In another set of experiment, WT macrophages were pre-treated for 1 h with a p38 inhibitor SB203580 (10 μM, Alexis Biochemicals, Plymouth PA) or a NF-κB inhibitor, Bay11-7082 (2 μM, Calbiochem, Darmstadt, Germany) [11] before addition to the top chamber while the lower chamber containing rMIF in DMEM (40 ng/ml, eBioscience, CA, USA). This concentration was reported as optimal for MIF mediated macrophage chemotaxis [12].

Generation of chimeric mice by bone marrow transplantation

Generation of chimeric model. Global MIFKO and WT mice (bone marrow recipients) were pre-conditioned with acidified water (pH 2-3) containing broad spectrum antibiotics Oxymav-B (120 mg/L) and Baytrill (50 mg/ml) for 2 days. Mice were irradiated twice with a dose of 550 Rads using a Gammacell 1000 Elite irradiator (Nordion International Inc.) at an interval of 3 h. Bone marrow from donor mice was harvested and suspended in DMEM supplemented with 10% FCS. Approximately 1×10^6 bone marrow cells were injected into each recipient mouse via the tail vein. Global MIFKO recipient mice received WT donor bone marrow to generate somatic-cell (or heart) MIF deficient mice (KO^{WT}), while WT recipient mice received MIFKO donor bone marrow to create bone marrow derived-cell (or leukocyte) MIF deficient mice (WT^{KO}). After bone marrow transplantation animals were allowed to recover for 4 weeks on acidified water and antibiotics as previously described [13].

Confirmation of bone marrow transplantation. In order to confirm the success of bone marrow transplantation and generation of chimeric mice, genomic DNA was extracted from whole blood collected from both KO^{WT} and WT^{KO} mice using Maxwell Whole Blood Purification Kits along with the Maxwell 16 Instrument (Promega, Madison, USA). Upon obtaining purified DNA, a standard genotyping protocol was followed (Online Figure 1).

Studies in chimeric mice. After 4 weeks recovery from BMT, chimeric mice were subject to coronary artery occlusion or sham operation. Echocardiography was performed prior to MI, 1 and 2 weeks following MI to assess LV dimensions and function using 1.7% isoflurane in air as previously described [5, 6]. Cardiac tissues were collected from sham operated and MI mice at various time points after surgery for gene expression of MIF, M1 macrophages markers [IL-1β, interferon-γ (IFN-γ), tumor necrosis factor α (TNFα), IL-6] and M2 macrophage markers [TGFβ1, arginase 1 (Arg-1), macrophage mannose receptor 1 (MRC-1) and CD163] [14] by qPCR. Immunohistochemistry for leukocyte infiltration and histological analysis were also performed for assessment of healing as aforementioned.

To clarify the potential effect of irradiation on observed phenotypes, we reconstituted WT bone marrow to irradiated WT mice (WT^{WT}), or global MIFKO bone marrow to irradiated MIFKO mice (KO^{KO}), then subjected these mice to coronary artery occlusion following the same protocol. Incidence of cardiac rupture was investigated for a period of 2 weeks.

Online Table 1. Echocardiographic data from WT and MIFKO mice following MI

	Prior to MI		1 week MI		4 weeks MI	
	WT	**MIFKO**	**WT**	**MIFKO**	**WT**	**MIFKO**
	n=18	n=22	n=12	n=15	n=12	n=14
HR	443±12	433±10	456±20	428±16	447±11	434±14
LVEDd (mm)	4.18±0.06	4.29±0.07	5.03±0.19*	4.65±0.14*	5.95±0.11*	5.17±0.16*†
LVEDs (mm)	2.78±0.06	2.67±0.05	4.07±0.21*	3.82±0.17*	4.82±0.18*	4.05±0.14*†
PWd (mm)	0.57±0.01	0.60±0.02	0.65±0.04	0.59±0.02	0.66±0.04	0.64±0.03
PWs (mm)	0.96±0.02	0.93±0.03	0.93±0.06	0.84±0.04	0.98±0.07	0.92±0.04
FS (%)	33.6±0.8	32.8±0.7	16.8±1.7*	20.6±1.5*	15.4±1.3*	19.7±1.1*†

Values are mean ± SEM, **P<0.05* vs. baseline, *†P<0.05* vs. WT.

WT, wild type; MIFKO, global MIF deficient mice; HR, heart rate; LVEDd, left ventricular end-diastolic diameter; LVESd, LV end-systolic diameter; PWd, LV posterior wall thickness at diastole; PWs, LV posterior wall thickness at systole; FS, fractional shortening.

References

[1] Fingerle-Rowson G, Petrenko O, Metz CN, Forsthuber TG, Mitchell R, Huss R, et al. The p53-dependent effects of macrophage migration inhibitory factor revealed by gene targeting. Proc Natl Acad Sci U S A 2003;100:9354-9.

[2] Gao XM, Ming Z, Su Y, Fang L, Kiriazis H, Xu Q, et al. Infarct size and post-infarct inflammation determine the risk of cardiac rupture in mice. Int J Cardiol 2010;143:20-8.

[3] Gao XM, Xu Q, Kiriazis H, Dart AM, Du XJ. Mouse model of post-infarct ventricular rupture: time course, strain- and gender-dependency, tensile strength, and histopathology. Cardiovasc Res 2005;65:469-77.

[4] Gao XM, Dart AM, Dewar E, Jennings G, Du XJ. Serial echocardiographic assessment of left ventricular dimensions and function after myocardial infarction in mice. Cardiovasc Res 2000;45:330-8.

[5] Gao XM, Liu Y, White D, Su Y, Drew BG, Bruce CR, et al. Deletion of macrophage migration inhibitory factor protects the heart from severe ischemia-reperfusion injury: a predominant role of anti-inflammation. J Mol Cell Cardiol 2011;50:991-9.

[6] Liu Y, Gao XM, Fang L, Jennings NL, Su Y, Q X, et al. Novel role of platelets in mediating inflammatory responses and ventricular rupture or remodeling following myocardial infarction. Arterioscler Thromb Vasc Biol 2011;31:834-41.

[7] Fang L, Gao XM, Moore XL, Kiriazis H, Su Y, Ming Z, et al. Differences in inflammation, MMP activation and collagen damage account for gender difference in murine cardiac rupture following myocardial infarction. J Mol Cell Cardiol 2007;43:535-44.

[8] Gao XM, Dilley RJ, Samuel CS, Percy E, Fullerton MJ, Dart AM, et al. Lower risk of postinfarct rupture in mouse heart overexpressing beta 2-adrenergic receptors:

importance of collagen content. J Cardiovasc Pharmacol 2002;40:632-40.

[9] Gao XM, Wong G, Wang B, Kiriazis H, Moore XL, Su YD, et al. Inhibition of mTOR reduces chronic pressure-overload cardiac hypertrophy and fibrosis. J Hypertens 2006;24:1663-70.

[10] Haudek SB, Xia Y, Huebener P, Lee JM, Carlson S, Crawford JR, et al. Bone marrow-derived fibroblast precursors mediate ischemic cardiomyopathy in mice. Proc Natl Acad Sci USA 2006;103:18284-9.

[11] Cheng Q, McKeown SJ, Santos L, Santiago FS, Khachigian LM, Morand EF, et al. Macrophage migration inhibitory factor increases leukocyte-endothelial interactions in human endothelial cells via promotion of expression of adhesion molecules. J Immunol 2010;185:1238-47.

[12] Bernhagen J, Krohn R, Lue H, Gregory JL, Zernecke A, Koenen RR, et al. MIF is a noncognate ligand of CXC chemokine receptors in inflammatory and atherogenic cell recruitment. Nat Med 2007;13:587-96.

[13] Kanellakis P, Slater NJ, Du XJ, Bobik A, Curtis DJ. Granulocyte colony-stimulating factor and stem cell factor improve endogenous repair after myocardial infarction. Cardiovasc Res 2006;70:117-25.

[14] Ma Y, Halade GV, Zhang J, Ramirez TA, Levin D, Voorhees A, et al. Matrix metalloproteinase-28 deletion exacerbates cardiac dysfunction and rupture after myocardial infarction in mice by inhibiting M2 macrophage activation. Circ Res 2013;112:675-88.

Online Figure Legends

Online Figure 1. Confirmation of bone marrow transplantation. Samples 1 and 2 are PCR products from WT and global MIFKO mice acting as controls while samples 3-6 represent PCR product from chimeric mice. PCR products for WT DNA are represented at 544 base pairs (bp) while global MIFKO DNA products are shown at 383 bp exhibiting a normal blood genomic profile. While irradiated WT mice with global MIFKO bone marrow engraphment demonstrated a MIFKO circulating genotype with PCR product at 383 bp. Conversely global MIFKO mice with WT bone marrow engraphment exhibited a WT genotype. This set of data confirms success of bone marrow transplant and establishment of chimeric models.

Online Figure 2. Global MIF deficiency had a modest influence in post-infarct healing. **A,** Representative images showing coagulative necrotic areas in infarct segments stained by hemotoxylin and eosin from WT and global MIFKO mice at 7 days after myocardial infarction (MI). Dot lines indicate the boundary of the necrotic area. **B,** Quantitative data of the necrotic area in the infarct region for the 2 groups at day-7 and day-14 after MI. **C,** Representative images of collagen deposition in the infarct region stained by picosirius red (red area) at day-14 following MI. **D,** Quantification of collagen density in the infarct region from both groups at 7 and 14 days post MI. **E**, Representative images of capillaries in the border zone by isolectin B4 staining (red colour) at day-7 after MI. **F,** Quantification of capillary densities in the border zones from WT and global MIFKO mice at day-7 and day-14 post MI. **G,** Temporal changes in mRNA level of TGFβ1 from WT and global MIFKO mice following MI. **H,** Changes in the infarct wall thickness between the 2 groups from 7 to 14

days following MI. ***P<0.05* vs. sham, †*P<0.05* vs. WT at the same time point. n=4 per sham group, n=7-8 per MI group.

Online Figure 3. MIF release from cultured cardiomyocytes (CM) or cardiac fibroblasts (CF) upon hypoxia stimulation and the influence of MIF in CF biology. A, *In vitro* cell culture study showing MIF released by both neonatal rat CM and CF after 6 hrs hypoxia detected by ELISA. The amplitude was significantly higher in CM than that in CF under the same cell densities. n=6 cell preparations per group. **P<0.01* vs. control (CTL). **B**, Cell proliferation expressed by CF counting in cultured CF (48 h) dissected from the day-4 infarct myocardium of global MIF deficient (KO) and wild type (WT) mice. n=8 cell preparations per group, **P<0.001* vs. day 0 (baseline), $^{\#}P<0.05$. **C**, Collagen deposition by cultured CF from the day-4 infarct myocardium of adult MIF KO and WT mice. n=5 per group, **P<0.001* vs. day 0. **D,** Fibrosis-related gene expression by cultured CF from the day-4 infarct myocardium of KO and WT mice. ***P<0.05* vs. WT, $^{\#}P<0.05$. n=5 per group.

Online Figure 4. Influence of bone marrow transplant on incidence of cardiac rupture in wild type (WT), reconstituted WT (WT^{WT}), global MIF deficient (KO) and reconstituted MIFKO (KO^{KO}) mice subjected to myocardial infarction (MI). A, Kaplan-Meier survival analysis of WT, MIFKO mice and KO^{KO} and WT^{WT} mice up to 2 weeks following MI. All sham operated animals survived (not shown). **B,** Cumulative incidence of cardiac rupture leading to mortality in WT, MIF KO and reconstituted WT^{WT} and KO^{KO} mice. Numbers in the bar represent the group size.

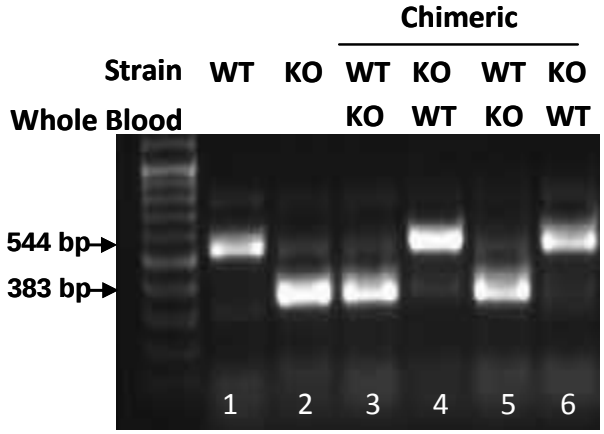

Online Figure 1

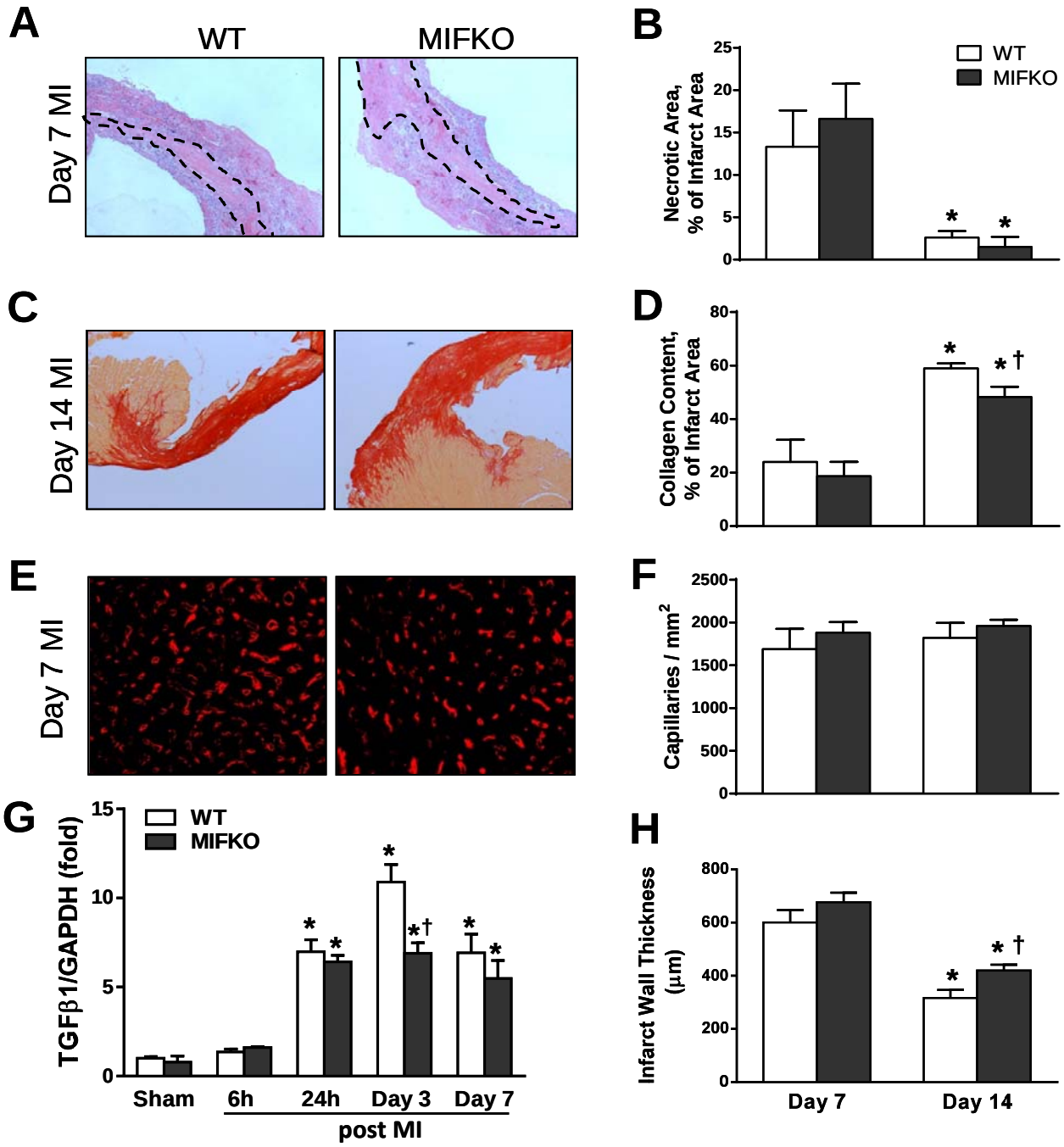

Online Figure 2

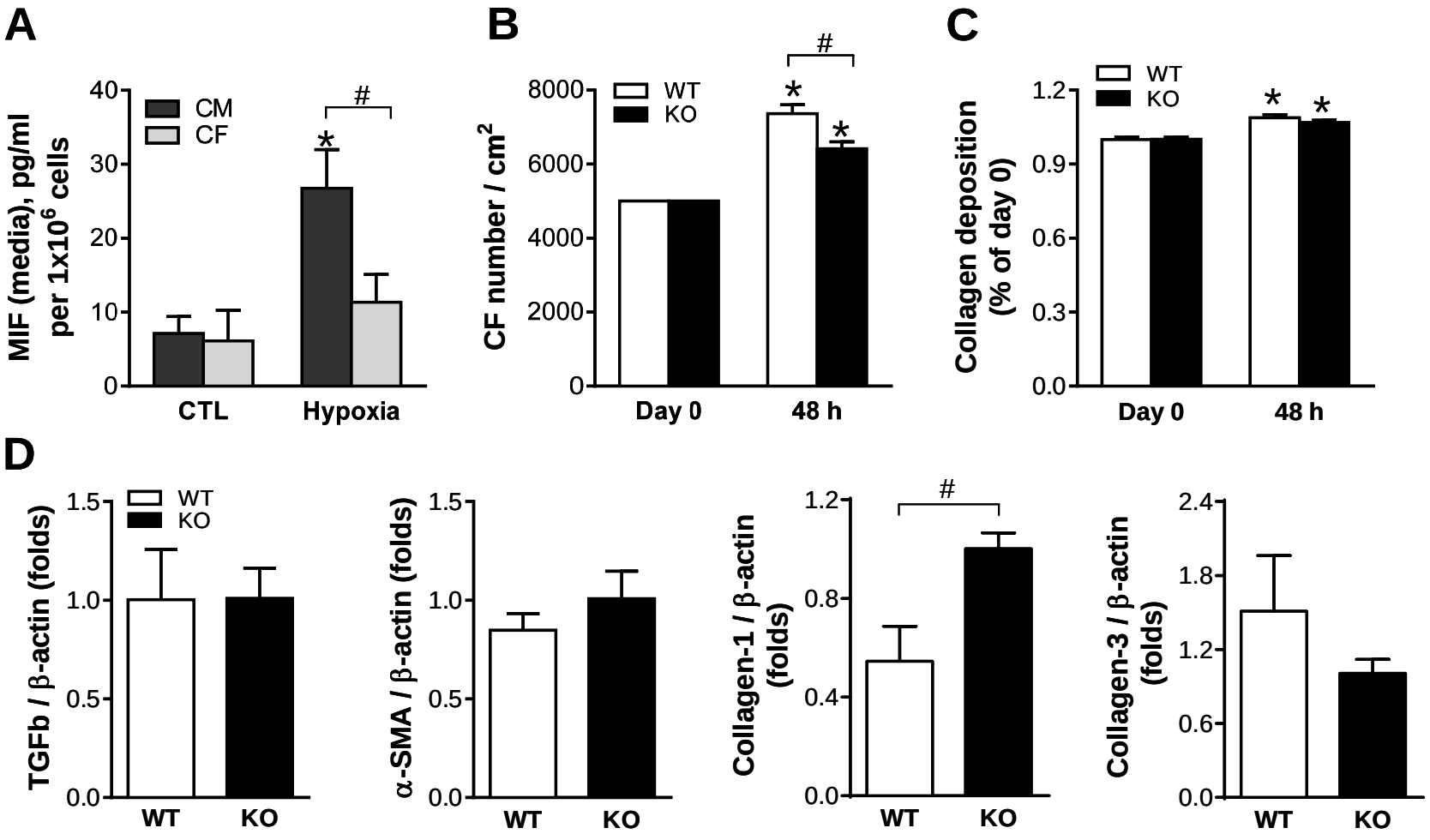

Online Figure 3

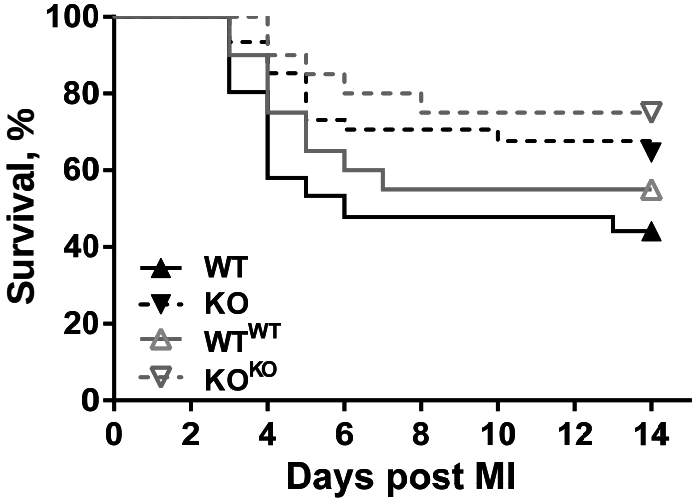

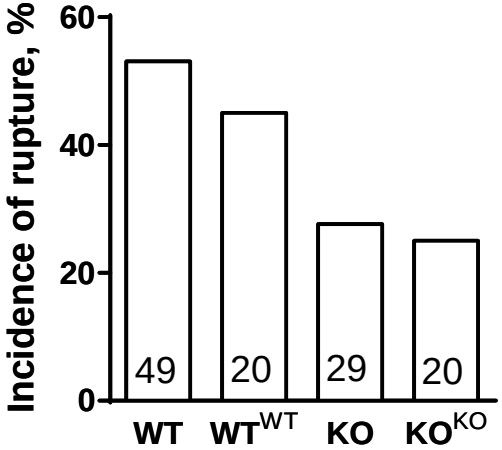

Online Figure 4